


# The role of StAR-D3 in HER2 overexpressing breast cancer

M.Sc. by Research
Teresa Mele

St Peter's College
MT 2011



***To my mother***

**Acknowledgements**

First of all I would like to thank my supervisors Prof. Alfredo Berruti and Prof. Luigi Dogliotti for offering me the opportunity to enjoy this wonderful experience which I will treasure both from a professional and personal point of view. The same applies to Dr. Alberto Bottini and Dr. Daniele Generali, who supported this idea with great enthusiasm from the very beginning.

I would also like to express my gratitude to my Oxford supervisors, Dr. Anthony Kong and Prof. Adrian Harris for their excellent guidance and suggestions throughout this challenging project.

I need to thank some special people who introduced me to the lab experience. First, Donatella, Guido, Valentina, Ida e Paolo for showing me, despite my skeptical thoughts, that magic things can happen within small tubes with invisible content. Moreover, all the lab members, particularly Merel for introducing me to the lab and for lots of suggestions and encouragement, especially when dealing with negative results, and Anassuya for precious explanations and suggestions in and out of the lab. Furthermore, Laura and Francesca for the biostatistics work and to Helen for staining suggestions.

I would also like to thank some special teachers who left their mark: Prof. Joseph Wilson, Prof. Lorenza Dellepiane, Prof. Sabrina Giannicchi.

I owe two people a special thank you: Cinzia for constant support (and for understanding in spite of silences and long distance), and Marco for surprisingly amazing and mind refreshing novels throughout the year.

Thanks for the little things which really made a difference: Chris and Ruben for keeping up with some well defined chocolate traditions, Ila and Carme for bits (too few) of nice times, Miguel for a broad spectrum of surprises, Nikos for

pumpkins and oxonian gooses, Michal and Pawel for climbing sessions, Philip's humour, Zoe's bits of poems and last but not least, Worcester college park.

A very special thank you goes to Marco and Francesca, Bean included of course, for the warmest welcome and pure nice times and to all the girls and guys from the "Fonderia" for being a source of inspiring enthusiasm (and cakes).

Thanks to Mel for her energy and sharing, and Simo for many reasons (too many to be listed here).

I am deeply grateful to my family for everything they taught me, especially for things they have not realized they did. Thanks for love, patience, support and constant encouragement.

## Abbreviations

ADCC: antibody dependent cellular cytotoxicity

AKT (PKB): Protein Kinase B

BSA: Bovine serum albumin

cDNA: complementary DNA

DAB: 3,3'-Diaminobenzidine

DARPP32: dopamine- and cAMP-regulated neuronal phosphoprotein

DMEM: Dulbecco's Modified Eagle Medium

dNTP: deoxyribonucleoside triphosphates

EGF: epidermal growth factor

EDTA: Ethylenediaminetetraacetic acid

EGFR: Epidermal Growth Factor Receptor

Fab: Fragment Antigen Binding

FACS: Fluorescence Activated Cell Sorting

FAS: Fatty Acid Synthase

Fc: Fragment Crystallizable

FBS: Fetal Bovine Serum

FISH: Fluorescence in situ hybridization

FITC: Fluorescein isothiocyanate

Fw: forward

GRB7: Growth factor receptor-bound protein 7

HER-2 / ErbB2: Epidermal Growth Factor Receptor 2

IHC: immunohistochemistry

Kb: Kilobase

LBPA: lysobiphosphatidic acid

MAPK/ERK: Mitogen-activated protein (MAP) kinases/extracellular signal-regulated kinases

MENTAL: Metastatic lymph node 64 N-Terminal

MENTHO: Metastatic lymph node 64 N-Terminal Homologue

MLN64: Metastatic lymph node 64

mRNA: messenger RNA

Mw: molecular weight

NK: Natural Killer cells

Opti-MEM: Opti-Minimal Essential Medium

PBS: Phosphate buffered saline

PBST: PBS Tween

PCR: Polymerase Chain Reaction

PFA: Paraformaldehyde

PI: Propidium Iodide

PNMT: phenyl ethanolamine N-methyltransferase

PS: Penicillin-Streptomycin

PVDF: Polyvinylidene Fluoride

qRT-PCR: Quantitative Real Time PCR

R-BT474: Trastuzumab Resistant BT474

RPMI medium: Roswell Park Memorial Institute medium

Rv: reverse

SD: standard deviation

siRNA: small interfering RNA

SRA: smallest region of amplification

StAR-D1: Steroidogenic Acute Regulatory Protein –Domain Containing Protein 1

StAR-D3: Steroidogenic Acute Regulatory Protein –Domain  Containing Protein 3

StAR: Steroidogenic Acute Regulatory Protein

START: StAR-related Transfer domain

TCAP: titin-cap

**Table of contents**

1. INTRODUCTION ..... 1

1.1 EGFR Family ..... 1

1.1.1 HER2: general characteristics ..... 1

1.1.2 Protein structure and signalling ..... 2

1.1.3 The ERBB2 Amplicon ..... 5

1.1.4 Targeted therapy: Trastuzumab ..... 7

1.1.5 Trastuzumab resistance ..... 8

1.1.6 HER2 network, lipids rafts and lipid metabolism ..... 10

1.2 StAR-D3 ..... 12

1.2.1 StAR-D3 and the START subfamily ..... 12

1.2.2 StAR ..... 14

1.2.3 StAR-D3 gene organization and transcriptional regulation ..... 15

1.2.4 StAR-D3 structure and function ..... 16

1.2.5 Clinical significance of StAR-D3 expression in breast cancer ..... 19

1.3 Aims and objectives ..... 21

2 MATERIALS AND METHODS ..... 22

2.1 MATERIALS ..... 22

2.1.1 Cell lines ..... 22

2.1.2 Solutions ..... 22

2.1.3 Reagents ..... 23

2.1.4 Drugs ..... 24

2.1.5 Oligonucleotides used in Quantitative Real Time PCR (qRT-PCR) ..... 24

2.1.6 Primary antibodies used for western blotting ..... 24

2.1.7 Secondary antibody used for western blotting ..... 25

2.1.8 Primary Antibodies for IHC ..... 25
2.1.9 Secondary Antibodies for IHC ..... 25
2.2 METHODS ..... 26
2.2.1 Cell culture ..... 26
2.2.2 Cell counting ..... 27
2.2.3 Protein extraction ..... 27
2.2.4 Protein quantification ..... 28
2.2.5 Western blotting ..... 29
2.2.6 Reverse transfection ..... 30
2.2.7 RNA procedures ..... 31
2.2.8 RNA extraction from cultured cells ..... 31
2.2.9 Nucleic acid quantification ..... 32
2.2.10 cDNA synthesis ..... 33
2.2.11 qRT-PCR ..... 33
2.2.12 Flow cytometry: FACS ..... 34
2.2.13 Cell Pellet Preparation ..... 35
2.2.14 Immunocytochemistry ..... 36
2.2.15 Biostatistics: gene expression analysis ..... 37
2.2.16 Statistical analysis ..... 37
3 RESULTS ..... 38
3.1 StAR-D3 and HER2 basal expression in HER2 amplified and non-amplified breast cancer cell lines ..... 38
3.1.1 StAR-D3 and HER2 gene expression ..... 38
3.1.2 StAR-D3 and HER2 protein expression ..... 39

3.2 The effect of StAR-D3 knockdown in HER2 amplified breast cancer cell lines.. 40
3.2.1 Optimisation of StAR-D3 knockdown assay in BT474 cells 40
3.2.2 BT474: StAR-D3 knockdown effect on HER2 expression 42
3.2.3 Effect of StAR-D3 knockdown on HER2 expression in SKBR3 cells.. 43
3.2.4 HER2 and StAR-D3 protein expression after StAR-D3 knockdown.. 44
3.3 Effect of StAR-D3 knockdown on cell survival in breast cancer cells 45
3.3.1 Effect of StAR-D3 knockdown on cell viability in MCF7 cells 45
3.3.2 StAR-D3 knockdown decreases cell viability in BT474 cells 46
3.3.3 Effect of StAR-D3 knockdown on apoptosis 47
3.3.4 Effect of StAR-D3 knockdown combined with Trastuzumab on cell survival 48
3.4 Effect of StAR-D3 knockdown combined with Trastuzumab on HER2 downstream effectors 50
3.5 Effect of StAR-D3 knockdown on Trastuzumab-resistant BT474 51
3.6 Gene expression analysis on HER2 positive breast cancer patients 52
3.7 StAR-D3 staining by immunocytochemistry on BT474 cell pellet 52
4 DISCUSSION 55
4.1 StAR-D3 and HER2 expression 55
4.2 StAR-D3 knockdown effects 55
4.3 Effect of StAR-D3 knockdown combined with Trastuzumab 56
4.4 Conclusion and future directions 57
5 REFERENCES 59

## List of figures

Figure 1-1……4

Figure 1-2……11

Figure 1-3……13

Figure 1-4……14

Figure 1-5……15

Figure 1-6……17

Figure 3-1……38

Figure 3-2……39

Figure 3-3……41

Figure 3-4……42

Figure 3-5……43

Figure 3-6……44

Figure 3-7……45

Figure 3-8……46

Figure 3-9……47

Figure 3-10……49

Figure 3-11……50

Figure 3-12……51

Figure 3-13……53

Figure 3-14……54

# 1. INTRODUCTION

## 1.1 EGFR Family

### 1.1.1 HER2: general characteristics

HER2 (epidermal growth factor receptor 2, also known as ErbB2/neu) belongs to the Epidermal Growth Factor Receptor Family, which also includes EGFR (Her 1), Her 3 and Her 4 [1].

Members of the Erbb family are closely related (40-45% identical to one another) type I transmembrane tyrosine kinase receptors which are involved in the regulation of a broad repertoire of cellular processes that mediate cell–cell interaction in organogenesis and adulthood. They control cell growth, survival, migration and differentiation, particularly important during embryogenesis [1,3].

Abnormal activation of these receptors is associated with a variety of human malignancies in terms of cancer development and progression, such as breast, gastric, ovarian and salivary glands cancer [1]. ERBB2 (neu/HER2) has been one of the most intensively studied receptors on this regard, due to its well-defined role in a particular subset of breast cancer [1,4,5].

HER2 amplification accounts for about 15-20% of invasive breast cancer and it defines a distinct biological entity within breast neoplasms, known to be associated with aggressive tumour behaviour (increased metastatic potential, shorter disease-free survival and overall survival) [6,7].

HER2 amplification occurs as an early event in the development of the malignancy, as it is overexpressed also in pre-neoplastic breast lesions such as atypical duct proliferations and in ductal carcinoma in situ [1].

For these reasons, HER2 has been proven a remarkable target for the treatment of HER2 overexpressing breast cancer [1,5].

### 1.1.2 Protein structure and signalling

HER2 is a 185 KDa transmembrane oncoprotein encoded by the HER2/neu oncogene, located on chromosome band 17q12.

Its structure is homologous to the other Erbb tyrosine kinase receptors, since the structural characteristics are highly conserved within the Erbb family members. The Erbbs have a ligand binding extracellular portion containing four domains (I, II, III and IV), a single transmembrane domain, a tyrosine kinase domain and a C-terminal tail which contains phosphorylation sites that serve as docking sites for downstream adaptors molecules containing SH2 or phospho-tyrosine binding domains [8,9].

At least 12 ligands are known to bind to Erbb receptors, including EGF and neuregulins (also known as heregulins). Ligand binding occurs at a site between domains I and III, it induces a dramatic conformational change in the receptor extracellular domain, hence causing dimerization and subsequent phosphorylation of highly conserved tyrosine residues within the receptor cytoplasmatic domain, which are docking sites for adaptor proteins and downstream effectors [3].

Ligand induced dimerization (which can occur as a homo-dimerization or hetero-dimerization, according to the Erbb members involved) is essential for receptor activation [10]. However, HER2 is the only member for which no ligand has been found: domain I and III are sterically in direct contact with each other, causing a closed position of the ligand binding site [10].

HER2 as a monomeric receptor does not have an autonomous kinase activity but it plays a pivotal role in cell signalling and has several peculiar characteristics within the EGFR family:

- it is the most favoured heterodimer partner of the EGFR family [1];
- HER2 can hetero-dimerize or directly cross talk with other partners not related to the EGFR family, such as the oestrogen receptor, IGF-1R or the angiogenic pathways [11,12];
- HER2 heterodimers undergo slow endocytosis, hence they have a longer lifetime on cell surface [13];
- although HER2 cannot bind any ligand, strong interaction between domains I and III leads to a constitutively extended dimerization arm resembling ligand-bound ErbB-1 [1]. It is therefore described as a 'promiscuous' receptor since it is always ready to dimerize [14];
- HER2 can only bind to a small subset of signaling molecules on its own [15];
- HER2 in partnership with other HER receptors can bind to a large subset of phosphor-Tyrosine binding proteins, therefore it has been defined as a *non-autonomous amplifie*r, capable of activating a potent mitogenic signal [14].

The downstream effect of HER2 signalling is not only to sustain cell proliferation, but also to influence several other essential mechanisms in cancer progression: angiogenesis, cell survival, apoptosis suppression, cell cycle control and cell motility via two major signalling pathways, MAPK and PI3K/AKT [1].

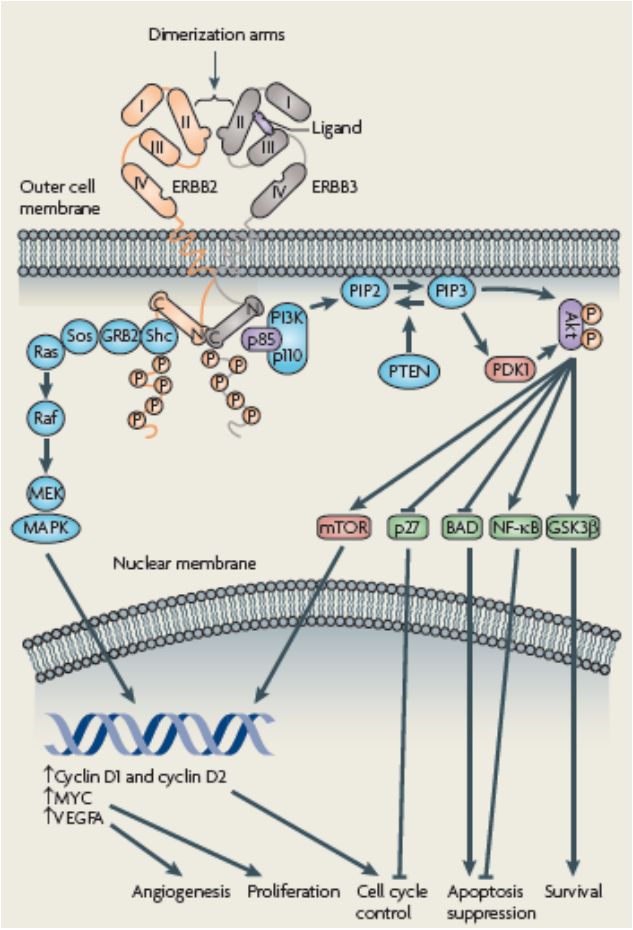



**Figure 1-1**

**HER2 downstream signaling. Dimer formation (homodimer or heterodimer) leads to cross-phosphorylation of dimer partners and results into multiple downstream cascades. MAPK pathway promotes cell proliferation, migration and angiogenesis. PI3K pathway leads to cell survival and apoptosis inhibition [1].**

### 1.1.3 The ERBB2 Amplicon

The "HER2 amplicon" is defined as the human chromosomal locus 17q12-q21, harbouring ERBB2 and a number of other relevant genes [16,17].

Over the years, in order to fully characterize the molecular consequences of the 17q12-q21 amplification, a few studies have evaluated the structure and the composition of the amplicon [17,18].

As described in Table 1-1 [19], these mapping efforts have been able to define a rather small *minimal core region of amplification* at the ERBB2 locus, also referred to as *SRA* (smallest region of amplification), spanning 633 kb [20].

Despite its small size, this region was demonstrated to contain a number of genes whose expression was almost consistently elevated in HER2 amplified breast cancer, such as GRB7 (Growth factor receptor-bound protein 7), PNMT (phenylethanolamine N-methyltransferase), DARPP32 (dopamine- and cAMP-regulated neuronal phosphoprotein), Telethonin or TCAP (titin-cap), MCG9753, MCG14832 and MLN64, also known as StAR-D3 [16,17].

Although HER2 amplification remains the primary and most common event in the 17q21 chromosome locus, it has been shown that several other genes are often amplified; among those, TOP2A (Topoisomerase 2-alpha), RARA (Retinoid acid receptor a) and GRB7 have been most extensively investigated [7].

Within this scenario, StAR-D3 seems to be invariably co-expressed and co-amplified with HER2 in breast and ovarian tumours, suggesting that, in addition to a localisation link, the two genes share a common transcriptional control. The promoters of both genes are positively regulated by Sp1 transcription factors [21].

However, for most of the genes included in the HER2 amplicon, the biological relevance and the subsequent clinical significance in breast cancer still need to

be unravelled. The hypothesis is that these co-located genes may influence expression and amplification of the HER2 oncogene, thereby influencing its clinical phenotype. Co-amplified and overexpressed genes may be involved in carcinogenesis, contributing to cell proliferation without inducing themselves cell transformation [7].

| Symbol | Alias | Description | Start bp position |
|---|---|---|---|
| **TRAF4** | **MLN62** | TNF receptor-associated factor 4 | 24095173 |
| **TIAF1** | | TGFB1-induced anti-apoptotic factor 1 | 24424665 |
| **MLLT6** | | Myeloid/lymphoid or mixed-lineage leukemia; translocated to, 6 | 34115412 |
| LOC284106 | | Hypothetical protein LOC284106 | 34140014 |
| **PCGF2** | **ZNF144** | Polycomb group ring finger 2 | 34143676 |
| **PSMB3** | | Proteasome (prosome, macropain) subunit, β type, 3 | 34162528 |
| PIP5K2B | | Phosphatidylinositol-4-phosphate 5-kinase, type II, β | 34177324 |
| RPL23 | | Ribosomal protein L23 | 34259865 |
| **LASP1** | **MLN50** | LIM and SH3 protein 1 | 34279894 |
| FLJ43826 | | FLJ43826 protein | 34439685 |
| PLXDC1 | | Plexin domain containing 1 | 34473083 |
| ARL12 | | ADP-ribosylation factor-like 12 | 34561546 |
| CACNB1 | | Calcium channel, voltage-dependent, β1 subunit | 34583235 |
| **RPL19** | | Ribosomal protein L19 | 34610096 |
| STAC2 | | SH3 and cysteine rich domain 2 | 34620316 |
| FBXL20 | | F-box and leucine-rich repeat protein 20 | 34670367 |
| **PPARBP** | **TRAP220** | PPAR-binding protein | 34816380 |
| **CRK7** | | CDC2-related protein kinase 7 | 34871818 |
| **NEUROD2** | | Neurogenic differentiation 2 | 35014575 |
| **PPP1R1B** | **DARPP-32** | Protein phosphatase 1, regulatory (inhibitor) subunit 1B | 35036705 |
| **STARD3** | **MLN64** | START domain containing 3 | 35046938 |
| **TCAP** | | Titin-cap (telethonin) | 35075125 |
| **PNMT** | | Phenylethanolamine N-methyltransferase | 35078033 |
| **PERLD1** | **MGC9753** | per1-like domain containing 1 | 35080902 |
| **ERBB2** | | v-erb-b2 erythroblastic leukemia viral oncogene homolog 2 | 35109922 |
| **C17orf37** | **MGC14832** | Chromosome 17 open reading frame 37 | 35138937 |
| **GRB7** | | Growth factor receptor-bound protein 7 | 35147744 |
| **ZNFN1A3** | | Zinc finger protein, subfamily 1A, 3 (Aiolos) | 35174724 |
| ZPBP2 | | Zona pellucida binding protein 2 | 35277995 |
| GSDML | | Gasdermin-like | 35314376 |
| ORMDL3 | | ORM1-like 3 | 35330822 |
| GSDM1 | | Gasdermin 1 | 35372752 |
| **PSMD3** | | Proteasome (prosome, macropain) 26S subunit, non-ATPase, 3 | 35390586 |
| CSF3 | | Colony stimulating factor 3 (granulocyte) | 35425214 |
| **THRAP4** | **TRAP100** | Thyroid hormone receptor associated protein 4 | 35428877 |
| **THRA** | **c-erbA** | Thyroid hormone receptor, α | 35472589 |
| **NR1D1** | | Nuclear receptor subfamily 1, group D, member 1 | 35502567 |
| **CASC3** | **MLN51** | Cancer susceptibility candidate 3 | 35550100 |
| RAPGEFL1 | | Rap guanine nucleotide exchange factor (GEF)-like 1 | 35591394 |
| WIRE | | WIRE protein | 35666238 |
| **CDC6** | | CDC6 cell division cycle 6 homolog | 35697672 |
| **RARA** | | Retinoic acid receptor, α | 35740896 |
| GJC1 | | Gap junction protein, χ 1, 31.9 kDa (connexin 31.9) | 35770433 |
| **TOP2A** | | Topoisomerase (DNA) II α 170 kDa | 35798321 |

**Table 1-1**

**List of genes in the 17q12-q21 region. The common region of amplification is indicated by dashed lines** [19]

### 1.1.4 Targeted therapy: Trastuzumab

The potential role of HER2 as a therapeutical target was first investigated in experiments in the early 1980's showing that monoclonal antibodies directed to the extracellular domain of the receptor determined a reduction in growth and a reduction in HER2 overexpressing in breast cancer cells [22].

Since then, further evidence has been obtained. Based on the increasing understanding of the role of the oncogene HER2 as a driving force towards disease progression, many efforts have been done in the latest years in the development of therapeutic agents that interfere with its function, and therefore with the downstream signalling of HER2.

Trastuzumab is a monoclonal antibody binding to domain IV of HER2 (juxtamembrane portion of HER2) consisting of a humanized IgG1 kappa light chain monoclonal antibody. Its mechanism of action is very complex and not fully understood yet. However, available data suggest that the effect of Trastuzumab depends on few main different mechanisms, not reciprocally related [7,23-25]:

- inhibition of signal transduction and cell cycle arrest;
- inhibition of PI3K/AKT pathway activation by activation of PTEN, leading to a cytostatic effect associated with G1 arrest; this effect is mediated by the Fab portion;
- Antibody Dependent Cellular Cytotoxicity (ADCC): it is a cell mediated immune response which plays a major role in Trastuzumab antitumoral effect. It is a process whereby the Fab region of an antibody binds to its specific antigen on a target cell, such as a cancer cell, whereas the Fc region engages with the Fc receptor present on the surface of effector

immune cells. Binding between the Fc region and its receptor triggers the activation of NK cells and degranulation of cytotoxic granules leading to cell death. The essential role of ADCC in Trastuzumab action was well elucidated by Clynes et al. who showed in animal models that Trastuzumab activity depended on the engagement of Fc receptor expressing lymphocytes: mice lacking the Fc effector function exhibited an impaired response to the monoclonal antibody[26] ;

- downregulation of surface HER2 by receptor mediated endocytosis;
- inhibition of proteolitic cleavage of the extracellular domain;
- inhibition of tumour angiogenesis (by downregulation of pro-angiogenic factors);
- inhibition of DNA damage repair.

Approved by the US Food and Drug Administration in 1998, Trastuzumab is now commonly used worldwide in metastatic, adjuvant and neoadjuvant setting, as clinical studies have established that the drug is active against HER2 overexpressing breast carcinomas [5,27].

### 1.1.5 Trastuzumab resistance

Despite the therapeutic successes obtained with Trastuzumab, drug resistance is common and significantly limits the potential of this treatment modality. When administered as a first line agent, it only achieves an objective response rate up to 34% for 9 months, whereas the remaining HER2 overexpressing carcinomas do not demonstrate any tumour regression (primary

or *de novo* therapeutic resistance). Moreover, some Trastuzumab-responding patients eventually develop resistance after continuous treatment and begin to progress again within one year (secondary or acquired resistance) [23,28].

As well as Trastuzumab mechanism of action, Trastuzumab resistance is a complex issue due to different mechanisms, such as:

1. obstacles in binding to HER2 (this may happen if HER2 is overexpressed in a truncated form, constitutively active or by means of epitope masking by molecules such as MUC4, a cell surface mucin) [23,28-30];
2. upregulation of downstream pathways: i.e. in presence of loss of function of PTEN, PI3K mutations [23];
3. upregulation of alternative downstream pathways which rescues cells from Trastuzumab-mediated cell growth inhibition, i.e. upregulation of IGFR, Met, Src [23,31-33];
4. failed ADCC [26];
5. HER2 activation via PKB-mediated feedback loop [34];
6. autocrine production of EGF-related ligands [29];
7. role of lipid rafts in terms of receptor lifetime on cell surface and its interaction with other molecules (i.e. EGFR-HER2 cross talk, integrins-growth factors cooperation in terms of decreased threshold of downstream signalling) [24,29,35].

The further identification in deep detail of these mechanisms could lead to the development of new compounds, which could overcome Trastuzumab resistance or could be used together with Trastuzumab to potentiate its action.

### 1.1.6 HER2 network, lipids rafts and lipid metabolism

The Erbb network is based on interaction of homodimers and heterodimers on the cell surface. In addition to these small-scale associations, higher order associations constituting of large clusters of HER2 in the cell membrane have also been identified (the diameter of HER2-rich membrane domains is about 0.5 μm, a size that increases upon HER2 activation [24]). These large-scale protein clusters are co-localized with ErbB3 proteins and lipid rafts [29].

Lipid rafts are membrane microdomains rich in cholesterol, sphingomyelin and glycolipids, insoluble in non-ionic detergents at 4°C. They participate in diverse cellular functions such as membrane trafficking, cell polarization, cell migration and receptor signalling (they can be considered as platforms either promoting or inhibiting downstream signalling) [24,28].

The relationship between lipid rafts and Trastuzumab resistance has been previously investigated by targeting an important enzyme involved in long-chain saturated fatty acid synthesis, namely Fatty Acid Synthase (FAS). The latter is also overexpressed in HER2 positive breast cancer. HER2 overexpression stimulates the FAS promoter and leads to an increase in endogenous fatty acid synthesis. Molecular cross talk between HER2 and FAS signalling pathways has been shown not only at transcriptional level but also at translational level and biosynthetic activity [36].

Moreover, FAS activity differs in normal cells compared to cancer cells. In normal cells it produces fatty acids from excess carbon, which are eventually stored as triglycerides. In cancer cells, FAS is mainly involved in producing phospholipids partitioning into lipid rafts aggregates.

Vazquez Martin et al. [37] showed that targeting fatty acid synthase-driven lipid rafts with siRNA leads to repression of HER2 at transcriptional level and attenuates its promoter activity, underlying a molecular link between FAS and HER2. On this basis, it has also been hypothesized that cancer associated FAS hyperactivity may play a role in determining the efficacy of Trastuzumab treatment, as shown in Figure 1-2 [28].

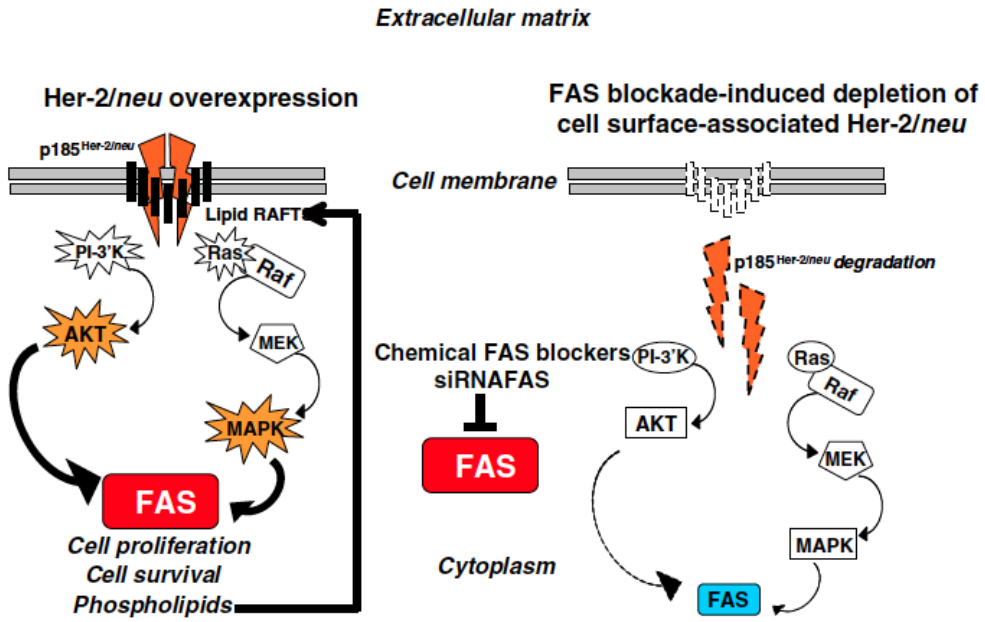



**Figure 1-2**

**FAS-regulated breast cancer cell sensitivity to Trastuzumab through the modification of lipid composition and functioning of the cell membrane in HER2 overexpressors.**

**Left panel: the bi-directional nature of the cross-talk between tumour-associated FAS and cancer-regulating proteins, such as HER2, strongly suggests that FAS actively contributes to the enhancement and maintenance of cancer phenotype. FAS activity plays also a major role in the synthesis of phospholipids partitioning into lipid rafts.**

**Right panel: co-localisation of lipid rafts and HER2, together with the lipid environment in the cell membrane of breast cancer cells profoundly influences the association properties and biological functions of HER2. FAS inhibition could induce a shift in the equilibrium between transport of HER2 to and from the membrane, favouring an increased internalization followed by intracellular degradation, thus enhancing the mechanism of action of Trastuzumab (adapted from Menendez et al. [28]).**

## 1.2 StAR-D3

### 1.2.1 StAR-D3 and the START subfamily

StAR-D3 (Steroidogenic Acute Regulatory Protein – Domain Containing Protein 3), also known as MLN64 (Metastatic Lymph Node 64), was originally identified by Tomasetto et al. [17] from a breast cancer-derived metastatic lymph node cDNA library by differential hybridization using malignant (hence MLN) versus non-malignant (breast fibroadenomas and normal lymph node tissue) breast tissue.

StAR-D3 cDNA encodes for a protein of 445 aminoacids that can be divided into two domains: the N terminal MENTAL (Metastatic lymph node 64 N-Terminal) domain and a C terminal START (StAR-related Transfer) domain, exposed to the cytoplasm [38].

StAR-D3 thus belongs to the START-domain containing proteins subfamily [2,39].

The START (StAR-related Transfer domain) domain is a protein domain spanning 200-210 amino acids motif, conserved through evolution through plants and animals. It serves as a versatile binding interface for lipids in many distinct biological processes including lipid transport, lipid metabolism and cell signalling [40-42] .

The human genome has 15 genes encoding START domains (Table 1-2), encoding for 15 proteins which have been found to contain a START domain, either alone or in combination with other domain [2].

| Name | Other names[a] | Lipid specificity[b] | Subcellular localization[c] | Expression pattern[d] | Mainly expressed[e] | Implicated in[f] | Gene chromosomal localization[g] |
|---|---|---|---|---|---|---|---|
| STARD1 | StAR | Cholesterol[1] | Mitochondria[1] | Specific | Adrenal, Gonads, Brain[1] | Genetic disorder[1] | 8p11.2 |
| STARD2 | PCTP | Phosphatidylcholine[2] | Cytosol[2] | Wide | | | 17q21-q24 |
| STARD3 | MLN64, CAB1 | Cholesterol[1] | Late-endosomes[3] | Wide | | ↑ Cancer[2] | 17q11-q12 |
| STARD4 | None | | Cytosol and Nucleus[4] | Wide | | | 5q22.1 |
| STARD5 | None | Cholesterol, 25-hydroxycholesterol[3] | Cytosol and Nucleus[5] | Wide | | ↑ Cancer[3*] | 15q26 |
| STARD6 | None | | Nucleus?[6] | Specific | Testis[2] | | 18q21.2 |
| STARD7 | GTT1 | | ? | Wide | | ↑ Cancer[4] | 2q11.2 |
| STARD8 | RhoGAP | | ? | Wide | Placenta, PNS | ↓ Cancer[5*] | Xq13.1 |
| STARD9 | None | | ? | Wide | | ↓ Cancer[6*] | 15q15.1-q15.2 |
| STARD10 | PTCP-like, SDCCAG28, CGI-52 | Phosphatidylcholine/ethanolamine[4] | Cytosol and Nucleus[7] | Wide | | ↑ Cancer[7] | 11q13 |
| STARD11 | CERT, GPBP, COL4A3BP | Ceramides[2] | Cytosol and Golgi[8] | Wide | | Autoimmune disease[8] | 5q13.3 |
| STARD12 | DLC-1,Arhgap7, p122-RhoGAP | | Plasma membrane[9] | Wide | | ↓ Cancer[9] | 8p22 |
| STARD13 | DLC-2, SDCCAG13 | | Cytosol?[10] | Wide | | ↓ Cancer[10] | 13q12-q13 |
| STARD14 | BFIT, THEA | | ? | Wide | | Obesity[11] | 1p32.3 |
| STARD15 | CACH | | Cytosol[11] | Specific | Liver, Lung | ↓ Cancer[12*] | 5q14.1 |

**Table 1-2**

**Human START- domain proteins** [2,39]

Phylogenetic analysis divides the family into six subfamilies (Fig. 1-3) [2,39].

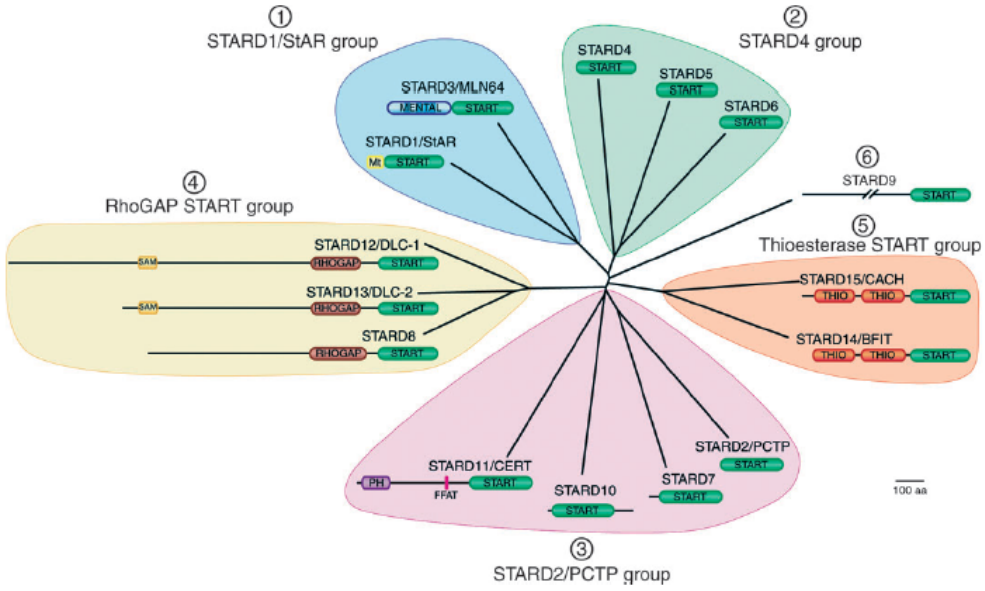



**Figure 1-3**

**Phylogenetic tree and domain organizations of the 15 START-domain proteins in humans** [2,39]

However, although START domains are found in a rather extensive protein family, lipid ligands have only been identified in a few cases[2], with StAR-D3 being one of them.

### 1.2.2 StAR

The prototype of START domain containing proteins, the function of most of which is still unclear, is StAR (Steroidogenic Acute Regulatory protein), also known as StAR-D1. StAR is a mitochondrial protein that regulates the limiting step in acute production of steroids in the adrenal cortex and gonads, in response to corticotropin and luteinizing hormone (Fig. 1-4), by transfering cholesterol from the outer to the inner mitochondrial membrane [41,43-45].

The structure, regulation, localisation and function of StAR are well known and characterized, since StAR mediates a critical transfer in steroidogenesis [41,44,45].

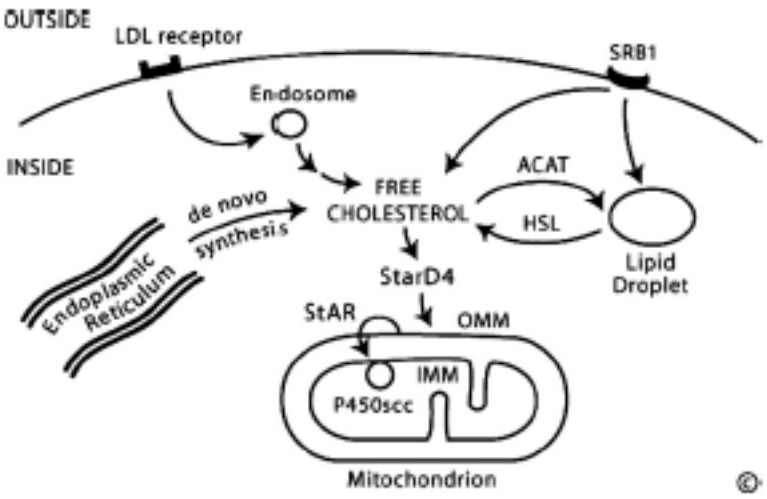



**Figure 1-4**

**StAR (StAR-D1) subcellular localization and mechanism of action [41].**

This explains how StAR deficiency causes congenital lipoid adrenal hyperplasia, a rare autosomal recessive disease characterized by steroidogenesis impairment and cholesterol deposits in steroidogenic tissues [41].

### 1.2.3 StAR-D3 gene organization and transcriptional regulation

Chromosomal mapping showed that the StAR-D3 gene is located in the q12-q21 region of the long arm of chromosome 17, in a centromeric position 30-40 Kb from HER2 [17]. Within this segment of the genome, several genes including StAR-D3 are invariably co-amplified and co-expressed with HER2 [18,46,47]. The characteristics of this gene-dense region and its clinical implications in carcinogenesis are described in Section 1.1.3.

The StAR-D3 gene is split into 15 exons located along 26 kb of genomic DNA. Exons 2-7 encode for the N-terminal MENTAL domain, whereas exons 9-15 encode for the C-terminal START domain (Figure 1-5) [21].

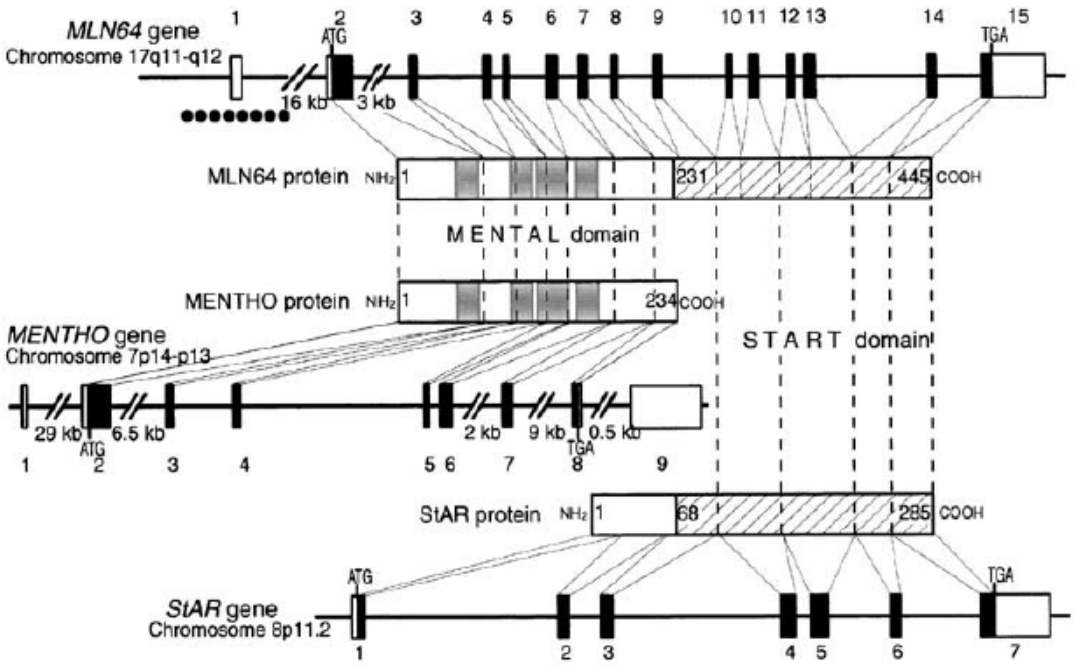



**Figure 1-5**

**Human MLN64, MENTHO and StAR (top, middle and bottom respectively) gene and protein organization. Coding exons are shown in black boxes, noncoding exons are shown in white boxes. Numbers in the protein domains represent amino-acid positions. The four transmembrane helices of the MENTAL and the START domains are indicated by grey and hatched boxes respectively.**

### 1.2.4 StAR-D3 structure and function

StAR-D3 was the second START domain protein to be characterized. It was originally identified in breast and ovarian cancers and it is the closest homolog to StAR (StAR-D1)[48].

As shown in Table 1-2, StAR-D3 is a widely expressed protein (not only confined to steroidogenetic tissues) with lipid specificity to cholesterol molecules, localized in late endosomes [49]. A complete co-localization of StAR-D3 was found with LBPA (lysobiphosphatidic acid), a marker of late endosomes, showing that it is a resident protein of such subcellular compartments [50,51].

StAR-D3 N terminus consists of a MENTAL domain which contains four potential transmembrane regions and targets the protein specifically to the membrane of late endosomes. It has been shown that if the MENTAL domain is removed, StAR-D3 becomes homogenously distributed throughout the cytoplasm [49].

StAR-D3 C terminus contains a START domain highly homologous to StAR-D1: StARD-3 and StAR-D1 share 35% sequence identity and about 60% amino-acid similarity in their START domain (C terminal) and have very similar biological functions [45,52].

Apart from lipid binding, a common feature of START proteins appears to be lipid exchange between membranes. The dynamics of this exchange are yet not fully unravelled but extensive studies on StAR raised some hypotheses and a potential model of action of this lipid transfer [2].

According to this model, StAR-D3 MENTAL domain anchors the protein at the periphery of late endosome membranes and captures cholesterol that is released from lipoproteins within the endosomal compartment whereas the

cytoplasmatic START domain extracts cholesterol prior to its transfer to an acceptor membrane, mainly mitochondria [2,53].

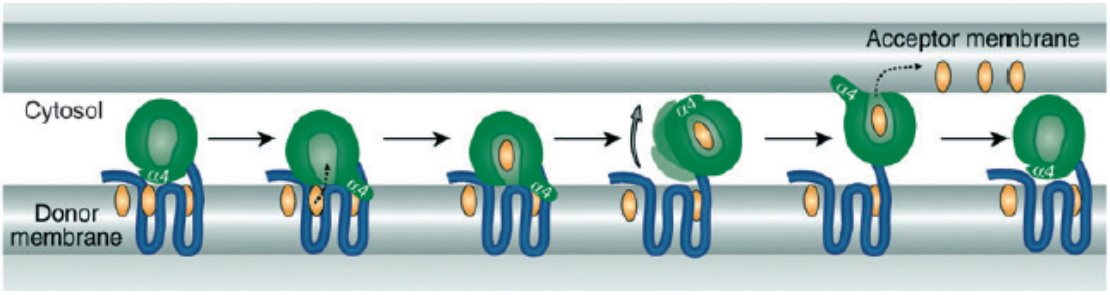



**Figure 1-6**

**MLN64 mechanism of action: the MENTAL domain (blue) anchors the protein to the endosomal membrane, leaving the START domain (green) in the cytoplasm. The START domain of MLN64 might work by extracting cholesterol (yellow) bound to its MENTAL domain from the late endosome membrane and transfer it to a closely positioned acceptor membrane [2].**

X-ray crystallography indicates that the START domain forms a hydrophobic tunnel structure that can bind a single cholesterol molecule. This tunnel must be intact for the biological activity of the domain (missense mutations of amino acids in this region are known to be responsible for congenital lipoid adrenal hyperplasia). The three-dimensional structure of the START domain of StAR-D3 and its ability to bind cholesterol (but not cholesterol esters) at an equimolar ratio have been described [45].

In addition to such structural homologies, it has been suggested that StAR-D3 and StAR may also have functional similarities, suggesting a potential role of StAR-D3 in mitochondrial cholesterol delivery [53].

However, StAR-D3 function remains mostly unclear and the main key-points in the literature can be summarized as follows:

- Watari et al. [52] showed that StAR-D3, as well as StAR, can enhance steroidogenesis in vitro;

- Zhang et al. [48] reported that truncated form of StAR-D3 (lacking the START domain) leads to free cholesterol accumulation in lysosomes and inhibits late endocytic dynamics;
- forced expression of a mutant StAR-D3 lacking the C terminal region induces a complete loss of steroidogenic activity; N terminal deletion results in enhancement of the stereodogenic activity [52];
- it has also been suggested that StAR-D3 can participate to steroidogenesis in tissues that do not express StAR, such as the placenta [52]. However, the full-length protein has negligible pro-steroidogenic activity and only a mutant form containing the isolated START domain significantly promotes steroid hormone synthesis [52,54];
- mouse model of StAR-D3 with selective removal of the START domain did not show any particular phenotype, suggesting that StAR-D3 is not critical for steroidogenesis [54];
- START domain has been shown to be a cholesterol binding domain for both proteins [45];
- according to further studies, StAR-D3 also has a role in actin-dependent fusion of late endosomes. Holtta-Vuori et al. [55] suggested that StAR-D3 overexpression enhances the fusion of late endosomes whereas StAR-D3 depletion results in the dispersion of late endocytic organelles.

### 1.2.5 Clinical significance of StAR-D3 expression in breast cancer

Little is known about StAR-D3 expression within malignancies and the clinical relevance of StAR-D3 in breast cancer has been poorly investigated. Even though the co-amplification of HER2 and StAR-D3 has been characterized in different settings, the actual expression in clinical samples has rarely been investigated. Currently, there are few reports regarding StAR-D3 expression in cancer patients and there are no reports on StAR-D3 expression in relation to any specific treatment [56,57] [58].

The milestone of StAR-D3 so far is its differential expression between neoplastic and normal tissue, since its overexpression in malignant tissues was confirmed in breast cancer and prostate cancer [58].

StAR-D3 transcripts were first identified by in situ hybridization in human breast tissues, within invasive carcinomas or in situ carcinomas (not within the stromal compartment or the normal epithelium). A similar expression pattern was also observed in metastatic lymph nodes: StAR-D3 expression was again limited to cancer cells only [49].

Such findings later led to the hypothesis that some hormone dependent tumours, such as prostate cancer, could use StAR-D3 by means of alternative steroidogenesis for self-maintenance, independently of circulating androgens. By analysing StAR-D3 expression by western blots and RT-PCR in 60 prostatic neoplasms, Stigliano et al. observed that StAR-D3 was present in the prostate homogenates of all patients studied but its expression was more evident in those patients carrying a high Gleason score (>7) [58]. StAR-D3 expression in neoplastic prostatic tissues was significantly higher than the normal tissue; interestingly, StAR-D3 was associated with high Gleason score, high stage and

short disease-free survival in prostate cancer [58], further confirming previous findings on breast cancer.

Cai et al. [56] analysed StAR-D3 expression in breast cancer samples by IHC and real time-PCR and correlated it with clinical and pathological data. Not only did they confirmed that StAR-D3 protein and transcript levels are significantly higher in neoplastic compared to normal tissue, but they also observed that StAR-D3 negatively correlates with clinical outcome (correlation with tumour spread, lymph node involvement, Nottingham Prognostic Index and overall survival). However, they did not specifically look at the prognostic role of StAR-D3 in HER2 positive breast cancer.

StAR-D3 analysis by RT-PCR, combined with HER2 RT-PCR analysis, was also investigated as a potential alternative to the current HER2 testing strategies in breast cancer. Vinatzer et al. [57] showed that combined scoring of StAR-D3 and HER2 with qRT-PCR is a promising complement or alternative to currently used IHC for HER2 testing, and that it also outperforms the prognostic accuracy of HER2 IHC and FISH.

The functional contribution of StAR-D3 in HER2 amplified breast cancer was first investigated by Kao et al. who reported that targeted knockdown of StARD3 resulted in a reduction in cell proliferation and cell cycle progression in SKBR3 and BT474 cells, albeit to a lesser extent than HER2 targeting. In their work they also analysed the effect of StAR-D3 knockdown on apoptosis in HER2 amplified cell lines, showing that StAR-D3 depletion led to increased apoptosis in SKBR3 as opposed to BT474 and MCF7 cells [59].

## 1.3 Aims and objectives

Taking into account all the previously described findings, particularly the co-expression of StAR-D3 and HER2 together with the effect of StAR-D3 depletion on cell proliferation and its unknown impact on apoptosis, this work aims to define more precisely the role of StAR-D3 in the biology of HER2 overexpressing breast cancer and its relation to Trastuzumab treatment.

The overall aims of this MSc thesis are:

1. to assess StAR-D3 expression in HER2 positive breast cancer cell lines;
2. to assess the role of StAR-D3 in relation to Trastuzumab treatment and resistance.

More specifically, the aims were investigated by:

- analysis of StAR-D3 expression in breast cancer cell lines;
- analysis of the effect of StAR-D3 knockdown on HER2 expression levels;
- analysis of the effect of StAR-D3 knockdown on cell survival and apoptosis (to further elucidate previous findings by Kao et al.[59]);
- analysis of a potential additive effect of StAR-D3 knockdown with Trastuzumab treatment in HER2 positive breast cancer cell lines;
- assessment of StAR-D3 expression levels in HER2 positive patients data sets;
- assessment of prognosis of StAR-D3 expression in a cohort of HER2 positive breast cancer patients.

# 2 MATERIALS AND METHODS

## 2.1 MATERIALS

### 2.1.1 Cell lines

The BT474, SKBR3 and MCF7 cells used in this work, listed in the table below, were provided by cell services at Cancer Research UK (Lincolns' Inn Fields laboratory). Trastuzumab-resistant cells were generated in our laboratory.

| Cell line | Origin | Culture medium |
|---|---|---|
| BT474 | Human Breast Ductal Carcinoma | RPMI 1640 |
| SKBR3 | Human Breast Carcinoma | DMEM |
| MCF7 | Human Breast Adenocarcinoma | DMEM |
| R-BT474 | Human Breast Ductal Carcinoma | RPMI 1640 |

### 2.1.2 Solutions

PBS: 137 mM NaCl, 2.7 mM KCl, 4.3 mM $Na_2HPO_4$, 1.4 mM $KH_2PO_4$, $Ca^{2+}$ and $Mg^{2+}$ free, pH 7.3

PBS-T: 0.2% (v/v) Tween 20 in PBS

4% PFA: 4% (v/v) PFA in PBS

Cell Lysis buffer: 20 mM Tris-HCl (pH 7.5), 10mM EDTA, 150 mM NaCl, 10 mM $Na_2P_2O_7$, 100 mM NaF, supplemented with 1% (v/v) Triton X-100 and 1 Complete Mini Protease Inhibitor Cocktail Tablet per 10 ml

Transfer buffer: 25 mM Tris, 192 mM glycine, 20% (v/v) methanol

Citrate buffer: 10 mM citric acid pH 6.0

Tris EDTA buffer: 50 mM Tris, 2 mM EDTA, pH 9.0

### 2.1.3 Reagents

| | Material | Source |
|---|---|---|
| Cell culture | RPMI 1640<br>DMEM<br>Opti-MEM® I Reduced Serum Medium, GlutaMAX™<br>Trypsin EDTA 0.5%/0.2% in PBS | Invitrogen |
| | FBS | PAA |
| Cell counting | ISOTON ® II diluent | Beckman Coulter |
| Cell lysis | Triton ® X - 100 | Sigma |
| | Complete Mini Protease Inhibitor Cocktail Tablets | Roche |
| Protein quantification | BIO-RAD Protein Assay | Biorad |
| Western blotting | β-mercapto ethanol | Sigma Aldrich |
| | Bovine serum albumin | Sigma Aldrich |
| | Restore™ PLUS Western Blot Stripping Buffer | Thermo Scientific |
| | NuPAGE® 4-12% Bis-Tris Gel 1.5mm x 10 wells | Invitrogen |
| | Immobilon®-P Transfer Membrane | Millipore |
| | 2.5 mm Blotting Filter Paper | Invitrogen |
| | NuPAGE® LDS Sample Buffer | Invitrogen |
| | NuPAGE® MOPS SDS Running buffer | Invitrogen |
| | ECL Detection Reagents | GE Healthcare |
| | Tween® 20 | Sigma Aldrich |
| | Novex® Sharp Protein Standard | Invitrogen |
| | Medical X-RAY Film | FUJIFILM |
| Cell transfection | Oligofectamine™ Reagent | Invitrogen |
| | StAR-D3 ON TARGET plus Smart Pool | Dharmacon |
| | Silencer® Negative Control #1 siRNA | Ambion |
| RNA extraction | Aurum Total RNA Mini Kit | Biorad |
| cDNA | 10X RT Buffer | Applied Biosystems |
| | 10X RT Random Primers | |
| | 25X dNTP Mix (100mM) | |
| | MultiScribe™ Reverse Transcriptase 50 U/µl | |
| PCR | Sensimix™ SYBR Mastermix (2x) | BIOLINE |
| FACS | FITC Annexin V Apoptosis Detection Kit I | BD Pharmingen |
| IHC | 2.5% Horse Serum Blocking Solution | Vector Laboratories |

### 2.1.4 Drugs

| Generic name | Trade name | Dose | Source |
|---|---|---|---|
| Trastuzumab | Herceptin | 40 µg/ml | Roche |
| Camptothecin | - | 6 µM | Sigma Aldrich |

### 2.1.5 Oligonucleotides used in Quantitative Real Time PCR (qRT-PCR)

| Primer | Oligonucleotide sequence | Primer Number | Source |
|---|---|---|---|
| StAR-D3 | Fw: 5'-TGC TCA GGA GCG GGA GTA-3' | S0172D03 | Invitrogen |
| | Rv: 5'-CAC GGT GTC CCC ATA TTC AT-3' | S0172D04 | |
| HER2 | Fw: 5'-TGC TGT CCT GTT CAC CAC TC-3' | S2050B12 | |
| | Rv: 5'-TCA TCC TCA TCA TCT TCA CAT TG-3' | S2050C01 | |
| β - actin | Fw: 5'-AAT GGC AAT GAG CGG TTC-3' | S2050B10 | |
| | RV: 5'-GGA TGC CAC AGG ACT CCA T-3' | S2050B10 | |

### 2.1.6 Primary antibodies used for western blotting

| Antibody | Species | Dilution and Molecular weight | Clonality | Source |
|---|---|---|---|---|
| MLN64 (ab3478) | Rabbit | 1:1000 53 KDa 1:500 | Polyclonal | Abcam |
| StAR-D3 antibody | Rabbit | 1:1000 50 KDa | Polyclonal | Novus Biologicals |
| β - actin | Rabbit | 1:2500 45 KDa | Polyclonal | Cell Signaling |
| HER2 | Rabbit | 1:1000 185 KDa | Polyclonal | |
| pAKT (S437) | Rabbit | 1:1000 60 KDa | Polyclonal | |
| pMAPK (T202-Y204) | Rabbit | 1:1000 44 KDa | Polyclonal | |

### 2.1.7 Secondary antibody used for western blotting

| Antibody | Species | Dilution | Source |
|---|---|---|---|
| ECL Anti-rabbit IgG | Donkey | 1:2500 | GE HealthCare |

### 2.1.8 Primary Antibodies for IHC

| Antibody | Species | Dilution | Source | Clonality |
|---|---|---|---|---|
| MLN64 (ab3478) | Rabbit | 1:100<br>1:250<br>1:500 | Abcam | Polyclonal |
| StAR-D3 antibody | Rabbit | 1:100<br>1:250<br>1:500 | Novus Biologicals | Polyclonal |
| MLN64 (D-20) | Goat | 1:100<br>1:250<br>1:500 | Santa Cruz Biotech | Polyclonal |

### 2.1.9 Secondary Antibodies for IHC

| **Antibody** | **Species** | **Source** |
|---|---|---|
| ImmPRESS™ Reagent Anti-Rabbit Ig | Goat | Vector Laboratories |
| Histofine® Simple Stain Anti-Goat Ig | Rabbit | Nichirei Biosciences |

# 2.2 METHODS

## 2.2.1 Cell culture

### 2.2.1.1 General growth conditions

Cells were grown in a tissue culture incubator in a humidified atmosphere of 5% CO2 and 95% filtered atmospheric air, maintained at a constant temperature of 37°C. Cells were cultured on sterile non-pyrogenic plastic ware (Cornig, USA), in 25 $cm^2$ and 175 $cm^2$ flasks with vented cap, 6 well plates, 24 well plates and 100 mm x 20mm dishes.

BT474 and R-BT474 were both cultured in Roswell Park Memorial Institute Medium 1640 (RPMI 1640), supplemented with 10% FBS and with 100 IU/ml Penicillin, 100 mg/ml Streptomycin (PS).

SKBR3 and MCF7 cells were cultured in Dulbecco's Modified Eagle Medium (DMEM) supplemented with 10% FBS and with PS (in the same concentration as in BT474).

R-BT474 cells were obtained by chronically treating BT474 cells with Trastuzumab 40 µg/ml in RPMI 1640 with 10% FBS and PS (100 IU/ml and 100 mg/ml) for six months.

#### 2.2.1.2 Subculturing

Cells were routinely subcultured when 90% confluent. Culture medium, PBS and trypsin/EDTA solutions were all pre-incubated in a 37°C water bath for 30 minutes. Medium was aspirated and discarded and the vessel was washed twice with PBS. 2 ml of trypsin/EDTA were then added to detach cells; the culture vessel was incubated at 37°C for 8 minutes to allow complete detachment of the cell layer up to single cell suspension. 20 ml of medium were used to neutralize the trypsin/EDTA. The cell suspension was then transferred to a 50 ml tube and centrifuged for 5 minutes at 1000 rpm. After centrifugation the medium was aspirated and discarded. The cell pellet was resuspended in 20 ml of medium and an appropriate volume of cells suspension was transferred in a new flask in 25 ml of fresh medium.

### 2.2.2 Cell counting

When an appropriate number of cells was needed in the setup of experiments, cells were detached, centrifuged and resuspended in an appropriate volume of medium. A volume of 19.6 ml of ISOTON ® II diluent (Beckman Coulter) was added to 400 µl of cell suspension in a sample vial. Cell counting was performed using a Z2 Coulter counter (Beckman Coulter) with cell size filters set to 9-27 µm. Cell counts provided a concentration of cells per ml.

### 2.2.3 Protein extraction

The following steps were performed on ice to reduce protease activity during the procedure. Medium was aspirated and cells were washed twice with

ice-cold PBS. Lysis buffer (section 2.1.2) was added to the cells (250 µl per 10 cm dishes, 100 µl per 6 well plates). Cells were scraped using a cell scraper (Corning) and the resulting lysate transferred to a 1.5 ml microcentrifuge tube. The lysate was centrifuged at 13500 rpm in a microcentrifuge for 10 minutes at 4° C to remove the cell pellet and the supernatant was stored at -80°C.

### 2.2.4 Protein quantification

Protein concentration was quantified using the Bio-Rad Protein Assay (Bio-Rad), based on the Bradford method (Bradford 1976) according to the manufacturer's instructions. The assay is based on the differential colour change of the dye according to different protein concentration.

The protein concentration of the cell lysate was determined using the Coomassie® Brilliant Blue G-250 dye which binds primarily to basic and aromatic amino acid residues (particularly arginine).

Serial dilutions of bovine serum albumin (BSA) were used as protein standards of known concentration to generate a standard curve. The dye was diluted with distilled water (1:5 ratio); 500 µl of diluted dye were then mixed with 2 µl of each standard or lysated sample and incubated for 10 minutes. A 200 µl duplicate of each sample was then transferred in a 96 well plate. The absorbance of the dye-protein complex was measured at 595 nm in a µQuant plate spectrophotometer (BioTek Intruments). The total protein concentration of the samples was derived from the standard curve using KC4 software (BioTek instruments).

### 2.2.5 Western blotting

Following protein quantification, the cell lysate was mixed (in 1:4 ratio) with a solution of 10% β-mercaptoethanol in NuPAGE® LDS Sample Buffer (Invitrogen). The samples were then boiled for 10 minutes at 95° C to dissociate the protein lysate into individual denatured polypeptide subunits. Equal amounts of protein, based on the Bradford assay, were loaded on to a precast NuPAGE® 4-12% Bis-Tris Gel and elecrophoresed in running buffer NuPAGE® MOPS SDS Running buffer (Invitrogen) at 130 V. Molecular weight markers (Novex® Sharp Protein Standard, Invitrogen) were run on gels to monitor electrophoresis, assess transfer efficacy and determine the approximate sizes of detected proteins. Separated polypeptides were then transferred onto a PVDF Immobilon®-P Transfer Membrane (Millipore) by semidry transfer. For each gel, the PVDF membrane was equilibrated with methanol and two sets of 2.5 mm Blotting Filter Paper were immersed in the transfer buffer (section 2.1.2) for 5 minutes. The protein gel was placed against a sheet of PVDF membrane, sandwiched between the two sets of paper and electrophoresed at 12V for two hours at room temperature. The membrane was then removed and washed with PBS. Unspecific binding sites were blocked by incubating the membrane for 1 hour at room temperature or overnight at 4 °C in blocking solution: 3% w/v BSA in PBST (0.2% v/v Tween 20 PBS).

To detect proteins, the membranes were incubated with primary antibodies (section 2.1.6) at the indicated dilutions either for 3 hours at room temperature or overnight at 4 °C. Following primary antibody incubation, the membranes were washed four times (10 minutes each) with 1% w/v low fat milk powder in PBST. The membranes were then incubated with the appropriate

secondary antibody (section 2.1.7) diluted 1:2500 in 5% w/v PBST for 1 hour at room temperature and washed four times (10 minutes each). Bound antibodies were detected using ECL Detection Reagents (GE Healthcare) followed by exposure to Medical X-RAY Film (FUJIFILM).

### 2.2.6 Reverse transfection

Culture medium, PBS, Opti-MEM and trypsin/EDTA solutions were all pre-incubated in a 37°C waterbath for 30 minutes. Volumes of reagents given are for a 6 well plate reverse transfection, per reaction. 3 µl of Oligofectamine™ Reagent (Invitrogen) were mixed with 12 µl of Opti-MEM and incubated for 5 minutes at room temperature. 2 µl of siRNA 20 µM (section 2.1.3) were mixed with 183 µl of Opti-MEM (final concentration of siRNA 20 nM); in the knockdown optimization 10 nM siRNA was also used following the same procedure. Diluted Oligofectamine was then added to each diluted siRNA and incubated for 20 minutes at room temperature to allow lipid-siRNA complexes to form. Media was aspirated and discarded from the culture vessel, followed by washing with PBS. Cells were trypsinized and incubated at 37°C for 10 minutes (up to single cell suspension). The trypsin was stopped by addition of an appropriate volume of culture medium. The cells were pelleted by spinning at 1000 rpm for 5 minutes and resuspended in fresh medium. After cell counting (Section 2.2.2) a cell dilution of 1.5 x $10^5$ cells/0.8 ml was prepared with 10% FCS medium without antibiotics. For each reaction, 200 µl of Oligofectamine/siRNA solution were added to 800 µl of cell suspension and incubated overnight. The culture media

was then replaced with 2 ml of fresh media without antibiotics (time considered as the baseline $t_0$ time point of the time course experiments).

### 2.2.7 RNA procedures

All solutions used for preparation and manipulations of RNA were prepared with nuclease-free water. Work surfaces were cleaned with RNase ZAP RNase decontamination solution (Ambion). Filtered pipette tips and sterile microcentrifuge tubes were RNase-free. Disposable nitrile rubber gloves were worn when handling RNA and samples were kept on ice at all stages of the procedures. RNA was routinely stored at -80° C.

### 2.2.8 RNA extraction from cultured cells

Total RNA was isolated from cultured cells using Aurum Total RNA Mini Kit (BIORAD) according to the manufacturer's instructions.

Cells were seeded at a density of 3 x $10^5$ per well in 6 well plates 48 hours prior to RNA extraction. If reverse transfected, cells were seeded at a density of 1,5 x $10^5$ per well. All the following steps were performed on ice.

The media was discarded and the cells rinsed twice with cold PBS and drained. Cells were then incubated with 350 μl of lysis solution, and then transferred into a RNA-binding column, within a 2 ml microcentrifuge tube. 350 μl of 70% Ethanol were added in the RNA column and the lysate was then centrifuged for 30'' at 10000 rpm. The filtrate was discarded and 700 μl of low stringency wash were added to the column. The column was centrifuged again for 30'' at 10000 rpm and the filtrate discarded. Next, 80 μl of diluted DNase I were added to the

column and incubated for 15 minutes at room temperature. The column was centrifuged for 30 '' at 10000 rpm and the filtrate discarded. 700 µl of low stringency wash were added and the column was centrifuged for 1 minute at 10000 rpm. The filtrate was discarded and the column was centrifuged again for 2 minutes at the same speed. The column was then transferred to a new microcentrifuge tube. To elute, 80 µl of elution solution (preheated at 70° C) were added on the membrane and incubated for 1 minute. The sample was then centrifuged for 2 minutes at 10000 rpm and the column discarded.

### 2.2.9 Nucleic acid quantification

Nucleic acid quantification was performed using the ND100 spectrophotometer supported by the NanoDrop Software (NanoDrop Technologies, USA). The sample pedestal was cleaned with distilled water before every use. A 2 µl sample of distilled water was placed on the sample pedestal to initialize the machine, as recommended by the manufacturer. 2 µl of elution buffer were used to blank the machine to prior measurements. The sample pedestal was wiped after every sample measurement with a clean Kim Wipe (Kimberly Clark, UK). A 2 µl sample of RNA was pipetted onto the sample pedestal for each reading. RNA was quantified using the DNA-40 presets. Assuming the weight of a nucleotide pair is 660 Da, the following formula was used: 1 unit A260 (absorbance 260nm) was equivalent to 40 µg/ml of RNA. The purity of DNA or RNA was assessed by the A260/A280 ratio and a value between 1.8 and 2.1 was considered pure.

### 2.2.10 cDNA synthesis

cDNA was synthesized using the High Capacity cDNA Reverse Transcription Kit (Applied Biosystems). For a 100 µl reaction, 50 µl of master mix (10 µl 10X RT Buffer, 4 µl 25X dNTPs, 10 µl 10X Random Primers, 5 µl MultiScribe™ Reverse Transcriptase and 21 µl RNase-free water) mix was added to 50 µl RNA (at a concentration of 1000 ng/µl or 800 ng/µl (according to the limiting sample). The solution was mixed and incubated for 10 minutes at 25° C, followed by two hours at 37° C. Samples were then kept at 4° C until storage at -20° C.

### 2.2.11 qRT-PCR

#### 2.2.11.1 Primers

Primers (Invitrogen) were resuspended in RNase-free water to give 100 µM stock solutions which were stored at -20° C. For qRT-PCR reactions 10 µM concentrations of primers were used.

#### 2.2.11.2 qRT-PCR Reactions

The following steps were performed on ice. Each qRT-PCR reaction required 10 µl Sensimix™ SYBR Mastermix (BIOLINE), 1 µl forward primer (10 µM), 1 µl reverse primer (10 µM), 3 µl RNase-free water and 5 µl cDNA. The cDNA concentration was calculated based on the concentration of RNA used in the reverse transcription reaction, assuming that it occurred at a 100% efficacy. Genes of interest (HER2 and StAR-D3) and the housekeeping gene were amplified in separate reactions and standard curves were run for every gene on

control template cDNA. Standard curves were used to analyse qRT-PCR reactions efficiency. Reactions were performed in triplicate using the Rotor Gene RG 3000 thermal cycler (Corbett Research) and the gene expression levels of each sample were normalized to β-actin.

The following profile was used for all the reactions: a hold at 95° C for 15 minutes, followed by 40 cycling runs (95° C for 10 seconds and 60° C for 1 minute) and a melt phase (from 50 to 99° C).

### 2.2.12 Flow cytometry: FACS

For evaluation of apoptosis 1.5 * 10^5 BT474 cells were reverse transfected (Section 2.2.6) and seeded in a 6 well plate prior to flow cytometric analysis. After an overnight growth interval in 10% FBS RPMI, the media was replaced and the apoptosis assessment was performed after 24 hours. As a positive apoptotic control, cells were treated with Camptothecin 6 mM for 12 hours. Untreated cells were used as negative control.

The following steps were performed on ice. Culture media was aspirated and kept in a 5 ml polypropylene round bottom tube (Falcon®). Cells were washed twice with PBS and detached by incubating at 37°C for 10 minutes in 0.5 ml trypsin/EDTA. PBS was merged with the media and the mix then used to block the trypsin reaction. Cells were pelleted by spinning at 1500 rpm at 4°C for seven minutes. After the removal of surnatant, cells were washed twice with cold PBS (4°C) and resuspended in 250 µl Annexin V Binding buffer (BD Pharmingen). 1 µl of PI and/or 1 µl of FITC Annexin V (BD Pharmingen) were added to the cell suspension. Samples were gently vortexed and incubated for 15 minutes in the

dark. 250 µl of Annexin V Binding buffer were added to each tube and samples were analysed by flow cytometry within one hour using a CyAN flow cytometer (Beckman Coulter). A typical viable cell area was gated and 20000 cells were counted. Analysis of results was performed using Summit 4.3 software (Dako Colorado).

### 2.2.13 Cell Pellet Preparation

BT474 cells were reverse transfected (Section 2.2.6) and seeded in 100mm x 20mm dishes. 48 hours after transfection (adequate time both for effectiveness of StAR-D3 knockdown and cell confluency of scramble sample) cells were trypsinized for 8 minutes at 37°C, resuspended in RPMI and centrifuged at 3000 rpm for 5 minutes. After removal of the medium cells were resuspended in 1 ml 4% PFA and fixed for two hours at room temperature. Cells were pelleted by centrifugation at 3000 rpm for 5 minutes and resuspended in 500 µl PBS. 2% agarose/formalin solution was melt in the microwave and then placed in 60°C water bath in order to allow the agarose to equilibrate. The cell suspension was also heated for 10 minutes at 60°C, then resuspended after the addition of 500 µl of agarose/formalin and quickly centrifuged in a vertical rotor. The tube was placed on ice, the gelled pellet was removed and the excess agarose was trimmed. The pellet was transferred in a pre-labelled tissue cassette and processed through an automatic tissue processor for paraffin infiltration of tissues in the Histopathology Laboratory of the John Radcliffe Hospital, Oxford. Following processing, the sample was embedded into a paraffin block. Four

micrometers sections were cut using a Leica RM 2135 microtome and placed on X-tra™ Adhesive slides (Leica) and air dried.

### 2.2.14 Immunocytochemistry

Cell pellet slides were placed in a metal slide rack and heated at 60°C for 10 minutes. They were dewaxed by immersing in Citroclear (HD Supplies) for 5 minutes twice, followed by 100 % Ethanol for 5 minutes twice, 50 % ethanol for 5 minutes and tap water for 5 minutes. Slides were then kept in PBS to avoid drying. Antigen retrieval was performed in a decloaking chamber (Biocare Medical) in citrate buffer Tris EDTA buffer (50 mM Tris, 2 mM EDTA, pH 9.0) or citrate buffer (10 mM citric acid pH 6.0).

The cell pellet on the slides was marked with a wax pen to maintain the antibodies on the sections, and all the incubations were performed in a humid slide box to decrease evaporation of the solutions. 15 minutes of incubation with 2.5% horse serum were performed to avoid unspecific binding of the primary antibody.

Primary antibodies (diluted 1:100, 1:250 or 1:500) were diluted in RMPI and incubated either overnight at 4°C or for two hours at room temperature. After two washes in PBS, slides were incubated with the secondary antibody (anti rabbit or anti goat) for 30 minutes at room temperature. Slides were washed with PBS and DAB was applied for 4-8 minutes. The slides were then immersed in PBS to stop the reaction and then counterstained in haematoxylin (Vector Laboratories) for 10''. After wash in tap water, coverslip were mounted on the section with Aquatex ® (Merck).

### 2.2.15 Biostatistics: gene expression analysis

A retrospective series of 219 patients with early primary breast cancer was considered; samples were collected from 2000 to 2005. StAR-D3 and HER2 gene expression was assessed in 198 patients with data for copy number (the complete patients' data set is fully described by Buffa et al. [60]).

Illumina ref8 Human array was used to interrogate mRNA expression for the analysis.

#### 2.2.15.1 mRNA expression probes

| Symbol | UniGene | Probe Id | Accession |
|---|---|---|---|
| StAR-D3 | Hs.77628 | GI_31543656-S 2650114 | NM_006804.2 |
| ERBB2 | Hs.446352 | GI_4758297-S 2350129 | NM_004448.1 |

Cyto-12 SNP arrays (Illumina) were used to assess the copy number data and the Onco-SNP algorithm was used to detect copy number changes [61].

Analyses were carried out using R Statistical Environment.

### 2.2.16 Statistical analysis

Prism 5 software (GraphPad Software) was used to generate the graphs and the statistical analysis.

# 3 RESULTS

For each presented figure, data were collected from three independent repeated experiments. Column bar graphs show mean ± SD.

## 3.1 StAR-D3 and HER2 basal expression in HER2 amplified and non-amplified breast cancer cell lines

StAR-D3 and HER2 basal expression was analysed both at gene level and protein level in HER2 amplified cell lines (BT474 and SKBR3) and in the control cell line (MCF7).

### 3.1.1 StAR-D3 and HER2 gene expression

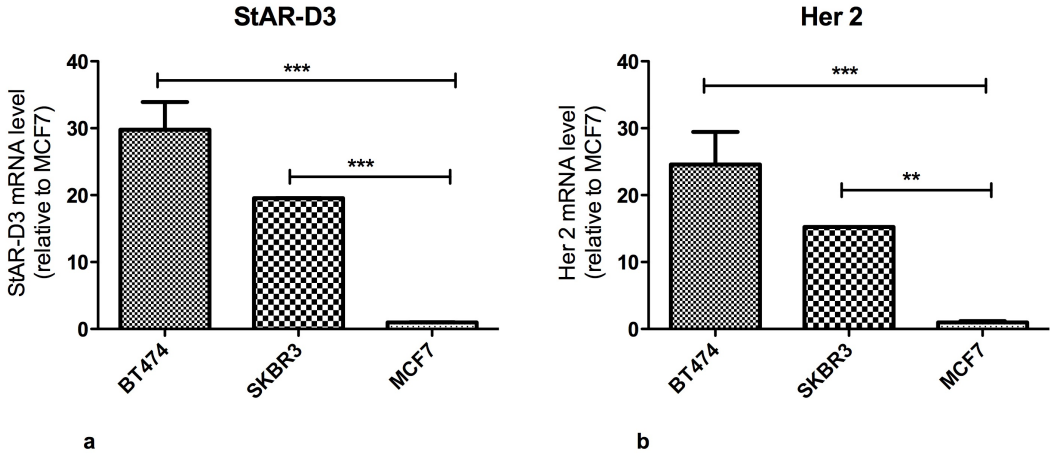



**Figure 3-1**

**StAR-D3 and HER2 expression in breast cancer cell lines. mRNA levels of BT474, SKBR3 and MCF7 cells respectively were assessed by qRT-PCR. Panels show StAR-D3 (a) and HER2 (b) mRNA levels respectively. Ratios are relative to mRNA levels of MCF7.**

Using qRT-PCR, it was shown that the relative gene expression of HER2 in BT474 and SKBR3 was significantly higher than in MCF7 (Figure 3-1). StAR-D3 gene showed a similar pattern of expression in the cell lines examined, as BT474 and SKBR3 both exhibited a significantly higher expression compared to MCF7 (Figure 3-1). Overall, both HER2 and StAR-D3 mRNA levels were higher in BT474 cells compared to SKBR3.

### 3.1.2 StAR-D3 and HER2 protein expression

The protein expression of StAR-D3 and HER2 was also assessed in baseline conditions in BT474, SKBR3 and MCF7 cells.

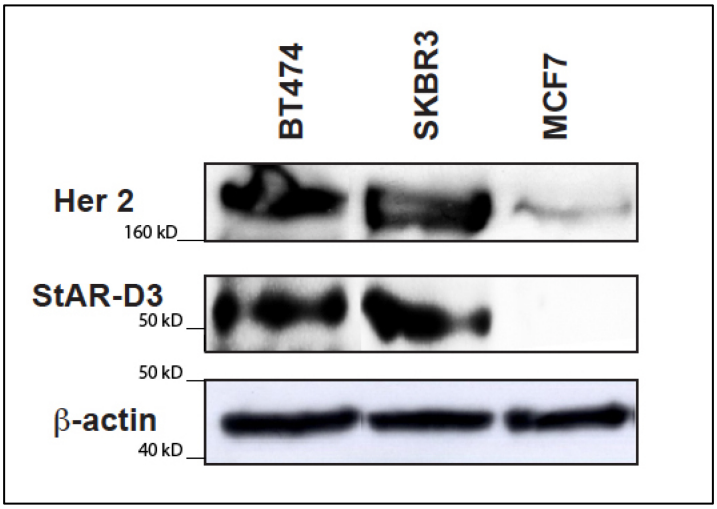



**Figure 3-2**

**StAR-D3 and HER2 expression in breast cancer cell lines. BT474, SKBR3 and MCF7 cells were lysed for Western blot analysis. Equal amounts of protein were loaded in each lane; membranes were blotted with antibodies for HER2, StAR-D3 and actin.**

Similarly to the previous findings on gene expression, HER2 amplified cell lines exhibited high levels of both proteins (HER2 and StAR-D3) in baseline conditions as opposed to MCF7 (in which StAR-D3 was not detectable and HER2 was expressed at a lower extent) (Figure 3-2).

## 3.2 The effect of StAR-D3 knockdown in HER2 amplified breast cancer cell lines

In order to assess the effect of StAR-D3 on different biological aspects in the examined breast cancer cell lines, StAR-D3 knockdown was performed by transient siRNA method.

StAR-D3 knockdown was carried out in BT474 cells, which harbour a higher level of HER2 in baseline conditions compared to SKBR3 cells. The siRNA knockdown of StAR-D3 was optimized in BT474 cells and its effect was also assessed in SKBR3. Thereafter, BT474 cells were used for the rest of the experiments presented in this thesis.

### 3.2.1 Optimisation of StAR-D3 knockdown assay in BT474 cells

To optimize the dose and duration required for the knockdown of StAR-D3 in BT474 cells, the cells were transfected with either specific siRNA, or control scramble siRNA, or mock solution. Different concentrations of StAR-D3 siRNA smart pool (Dharmacon) were used to assess the optimal knockdown (Section 2.2.6).

After StAR-D3 knockdown, StAR-D3 mRNA levels significantly decreased both at 24 and 48 hours at both siRNA concentrations. When [10 nM] siRNA was used the knockdown was significant. However, [20 nM] siRNA led to a higher and more sustained reduction of mRNA in BT474 cells, hence the optimal assessed concentration of siRNA was deemed to be 20 nM and it was further used in subsequent experiments.

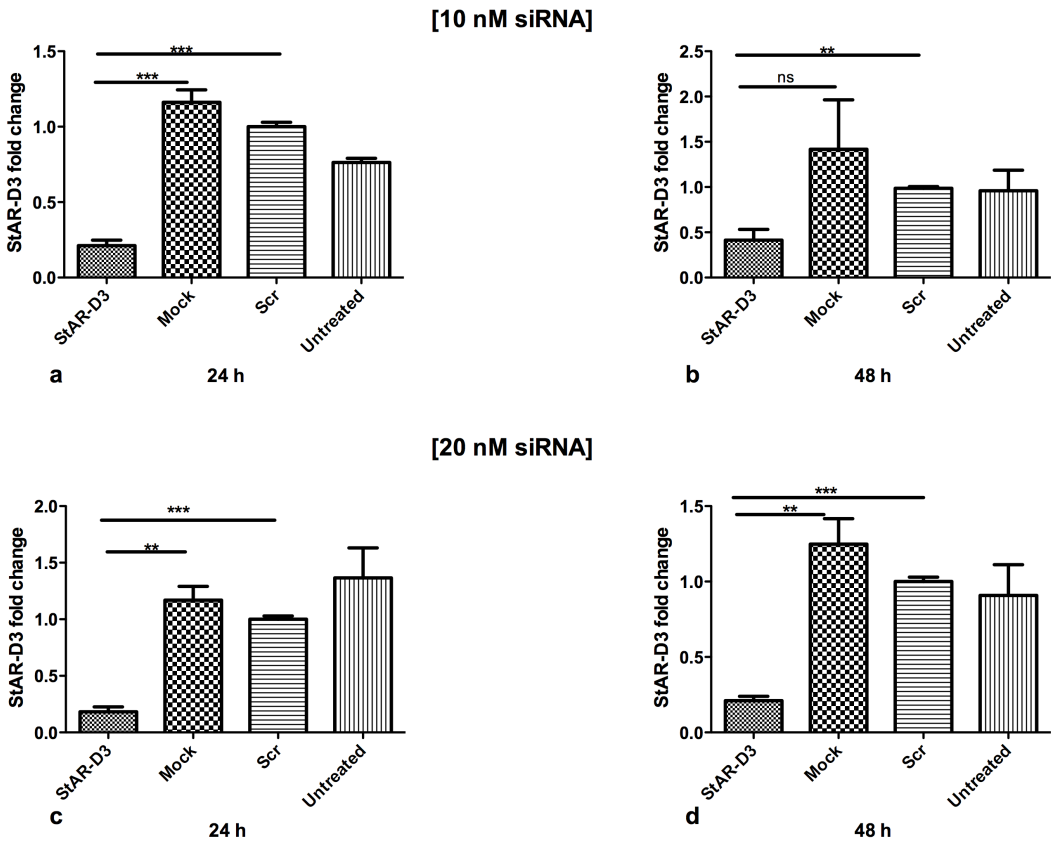



**Figure 3-3**

**StAR-D3 knockdown assay in BT474 cells. qRT-PCR assessed mRNA levels of StAR-D3 are shown in the siRNA transfected cells compared to mock or scramble control siRNA cells**

**siRNA pooled StAR-D3 was used at 10 nM (a) and (b) or 20 nM (c) and (d). mRNA was extracted at 24 hours (a) and (c) or 48 hours (b) and (d).**

### 3.2.2 BT474: StAR-D3 knockdown effect on HER2 expression

The effect of StAR-D3 knockdown on HER2 expression was analysed, given the frequent co-expression of StAR-D3 and HER2, being both in chromosome 17.

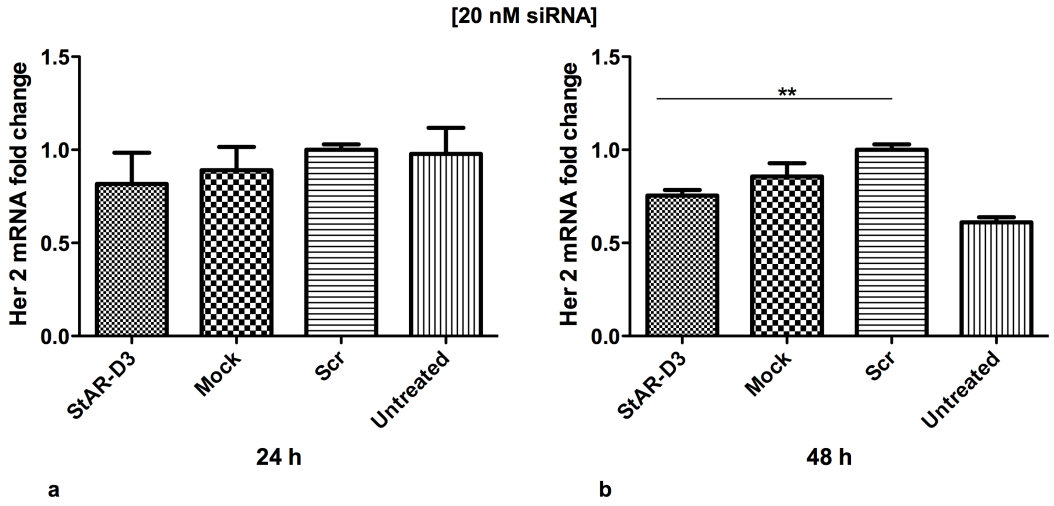



**Figure 3-4**

**StAR-D3 knockdown effect on HER2 expression in BT474 cells. qRT-PCR assessed mRNA levels of HER2 are shown in the siRNA transfected cells compared to mock or scramble control siRNA cells.**

**siRNA pooled StAR-D3 was used at 20 nM. mRNA was extracted at 24 hours (a) and 48 hours (b).**

In BT474 cells, HER2 expression was decreased at 48 hours from StAR-D3 knockdown (Figure 3-4). However, such downregulation of HER2 mRNA was less evident than the one observed in SKBR3, as shown in next section 3.2.3.

HER2 reduction could be due to a common regulation shared between HER2 and StAR-D3 or could be determined by an off target effect of StAR-D3 knockdown, hence leading to a false positive result.

In order to minimize the latter hypothesis, siRNA titration was performed and cells were transfected with a scramble non targeting negative control siRNA.. The detection of siRNA effects on unintended targets by rescue experiments (restoring the native phenotype by expressing a functional version of the target

gene which is resistant to the silencing siRNA) was not performed, due to time constraints.

### 3.2.3 Effect of StAR-D3 knockdown on HER2 expression in SKBR3 cells

After optimising the dose and duration required for the knockdown of StAR-D3 in BT474 cells, the same conditions were used in SKBR3 cells. In SKBR3 cells StAR-D3 knockdown was effective, showing a significative reduction of StAR-D3 mRNA levels compared to the control samples. Similarly, StAR-D3 knockdown led to a reduction of HER2 mRNA levels (Figure 3-5). However, the extent of StAR-D3 knockdown was lower than the one observed in BT474.

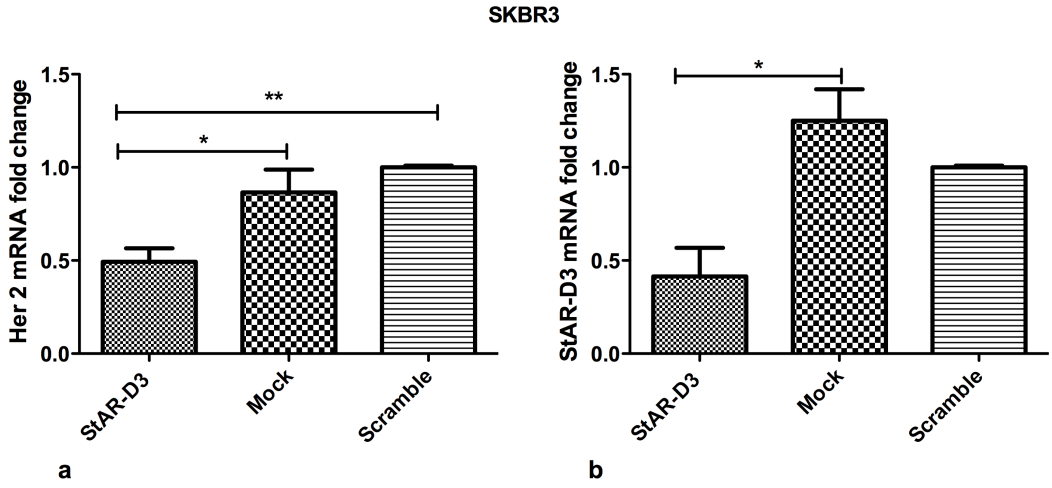



**Figure 3-5**

**StAR-D3 knockdown leads to a decrease in HER2 expression in SKBR3 cells. siRNA pooled StAR-D3 was used at 20 nM and mRNA was extracted at 48 hours.**

**qRT-PCR assessed mRNA levels of HER2 and StAR-D3 are shown: (a) HER2 expression in StAR-D3 knockdown cells compared to mock or scramble control siRNA cells; (b) StAR-D3 mRNA expression in the specific siRNA transfected cells compared to mock or scramble control siRNA cells .**

### 3.2.4 HER2 and StAR-D3 protein expression after StAR-D3 knockdown

To further prove the effectiveness of StAR-D3 knockdown, protein levels of StAR-D3 were assessed. As shown in Fig. 3-6, StAR-D3 protein levels in the specific siRNA-transfected sample were lower than in the controls, in accordance with the previous data on gene expression. HER2 expression was also slightly reduced when StAR-D3 was knocked down in BT474 cells.

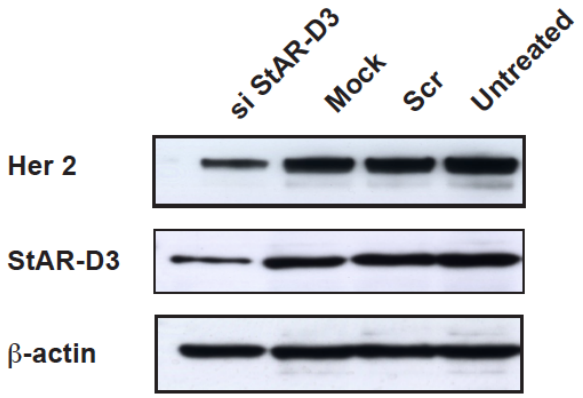



**Figure 3-6**

**Effect of StAR-D3 knockdown on StAR-D3 and HER2 protein levels in BT474 cells.**

**Cells were transfected with 20 nM pooled siRNA against StAR-D3 or a scramble sequence. The knockdown was validated by western blot for StAR-D3 and β-actin and HER2 protein levels were also assessed. Equal amounts of protein were loaded in each lane and membranes were blotted with appropriate antibodies for HER2, StAR-D3 and β-actin.**

## 3.3 Effect of StAR-D3 knockdown on cell survival in breast cancer cells

To further investigate the role of StAR-D3 in HER2 amplified breast cancer cell lines, cell survival was analysed after StAR-D3 knockdown. MCF7 cells, carrying low levels of StAR-D3 both at gene level and protein level, were used as the control cell line.

### 3.3.1 Effect of StAR-D3 knockdown on cell viability in MCF7 cells

Cell viability was assessed via cell count evaluation at different timepoints after StAR-D3 knockdown in MCF7. In si-StAR-D3 samples the cell count was slightly lower than in the control samples in all the timepoints examined (Figure 3-7). However, the difference was not statistically significant.

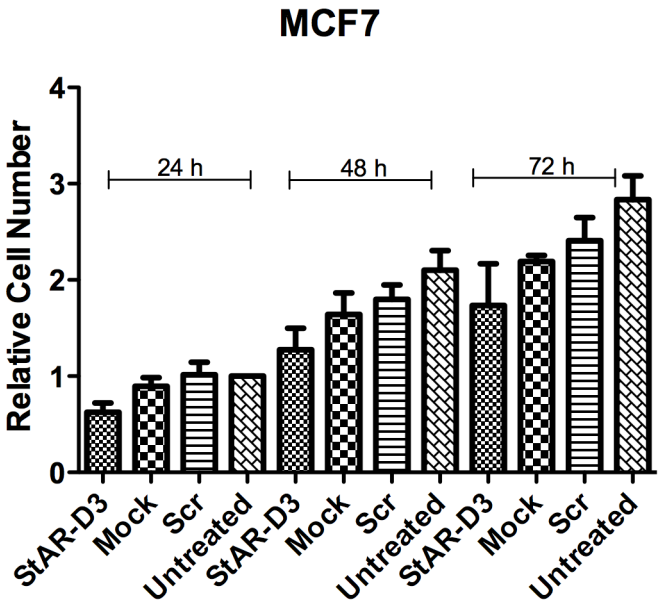



**Figure 3-7**

**Effect on cell viability by si-RNA mediated StAR-D3 knockdown in MCF7 cells.**

**MCF7 cells were transfected with 20 nM pooled siRNA against StAR-D3. Cell viability was assessed 24, 48 and 72 hours from reverse transfection, respectively. Transfections were performed in triplicates and the plotted bars show the cell viability, relative to the untreated cells. Cell viability was assessed as described in section 2.2.2**

### 3.3.2 StAR-D3 knockdown decreases cell viability in BT474 cells

After StAR-D3 knockdown, cell viability was assessed in BT474 cells, which harbour higher levels of StAR-D3 both at protein and gene level in basal conditions as opposed to MCF7 cells. When StAR-D3 expression was lowered, BT474 cell count dropped dramatically as opposed to the control conditions (Figure 3-8). The difference in cell viability was statistically significant and it was particularly noticeable in the latest timepoint considered.

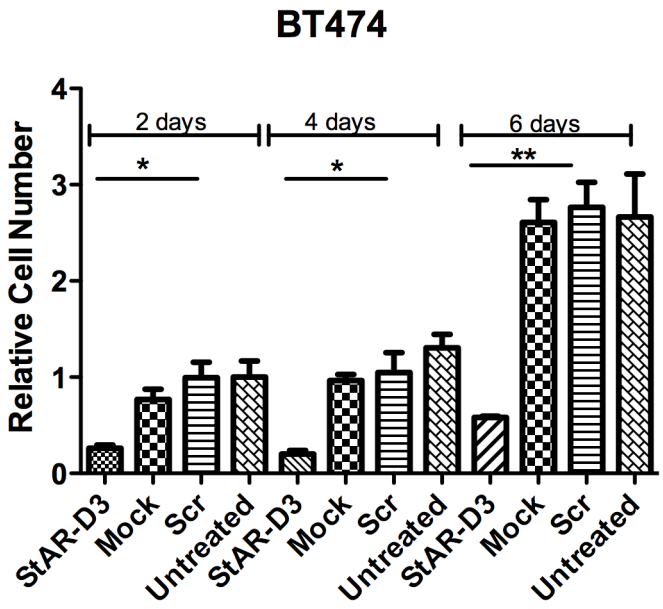



**Figure 3-8**

**Effect on cell viability by si-RNA mediated StAR-D3 knockdown in BT474 cells.**

**BT474 cells were transfected with 20 nM pooled siRNA against StAR-D3. Cell viability was assessed after 2, 4 and 6 days respectively. Transfections were performed in triplicates and the plotted bars show the cell viability, relative to the untreated cells. Cell viability was assessed as described in section 2.2.2.**

### 3.3.3 Effect of StAR-D3 knockdown on apoptosis

To determine whether the decrease in cell viability was attributable to apoptosis, BT474 cells were stained with FITC conjugated Annexin V and PI and evaluated by FACS analysis. As described in section 2.2.12, the apoptotic positive control was treated with Camptothecin 6 μM and the analysis was carried out at a 24 h timepoint. Since Annexin V staining depends on the loss of membrane integrity which accompanies cell death in apoptotic processes, early apoptotic cells were identified as being Annexin V positive and PI negative (PI is normally excluded in viable cells). Fully viable cells were identified as both Annexin V and PI negative, as opposed to dead cells both Annexin V and PI positive.

Compared to the scramble control, StAR-D3 depleted cells showed a significantly higher percentage of apoptotic cells (15.5 % ± 1.5 versus 4.28% ± 0.1, $p<0.05$), suggesting a potential role of StAR-D3 in maintenance of cell survival.

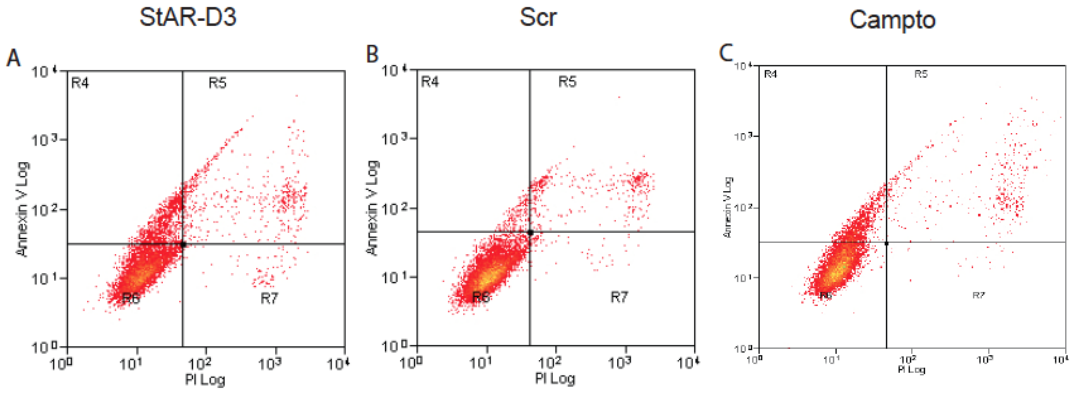



**Figure 3-9**

**StAR-D3 knockdown induces increased apoptosis in BT474 cells.**

**BT474 cells were transfected with 20 nM pooled siRNA against StAR-D3. As described in Section 2.2.12, FACS analysis was performed 24 hours after transfection. The panels show Annexin V and PI staining. Early apoptotic cells are shown as Annexin V positive and PI negative in (a) si-StAR-D3 (b) Scramble and (c) Camptothecin treated samples respectively.**

### 3.3.4 Effect of StAR-D3 knockdown combined with Trastuzumab on cell survival

To further investigate the role of StAR-D3 in HER2 driven biology and in response to HER2 targeted therapy, the impact on cell survival of StAR-D3 knockdown in addition to Trastuzumab treatment was also analysed.

As shown in section 3.3.2, StAR-D3 knockdown in BT474 led to a decrease in cell proliferation, in particular after 24 hours from transfection, which appeared to be partially due to apoptosis.

To address whether StAR-D3 depletion could also enhance Trastuzumab sensitivity in BT474 cells, cellular viability was assessed after StAR-D3 knockdown and Trastuzumab treatment. Samples were reverse transfected and treated with Trastuzumab 40 μg/ml for 24, 48 and 72 hours respectively.

Trastuzumab treatment alone did not inhibit cell viability of BT474 cells in any of the time points (Figure 3-10). StAR-D3 knockdown alone induced a significant decrease in cell viability at 48 hours and 72 hours (Figure 3-10).

StAR-D3 depleted samples treated with Trastuzumab showed a trend to a lower percentage of viable cells compared to StAR-D3 depleted only. However the two samples did not show any significant difference (assessed by one-way ANOVA).

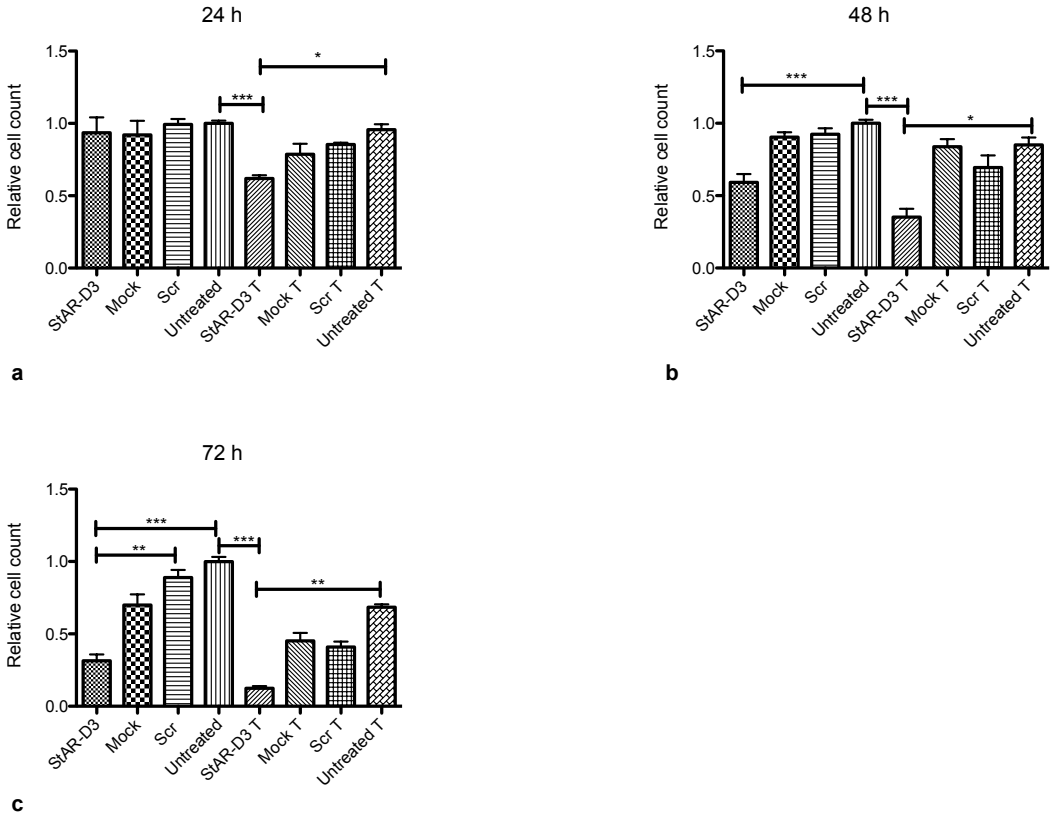



**Figure 3-10**

**Effect of si-RNA mediated StAR-D3 knockdown combined with Trastuzumab treatment on BT474 cells. Cell viability was assessed 24 h (a), 48 h (b) and 72 h (c) after transfection respectively; T-labelled samples were treated with Trastuzumab (40 μg/ml). Transfections were performed in triplicates and the plotted bars show the cell viability, relative to the untreated cells. Cell viability was assessed as described in section 2.2.2.**

## 3.4 Effect of StAR-D3 knockdown combined with Trastuzumab on HER2 downstream effectors

StAR-D3 knockdown resulted in a downregulation of pAKT and pERK, both of which are HER2 downstream effectors (Figure 3-11). When StAR-D3 knockdown was combined with Trastuzumab treatment, there was a further downregulation of pAKT level, correlating with a greater inhibition on cell viability from combined treatment.

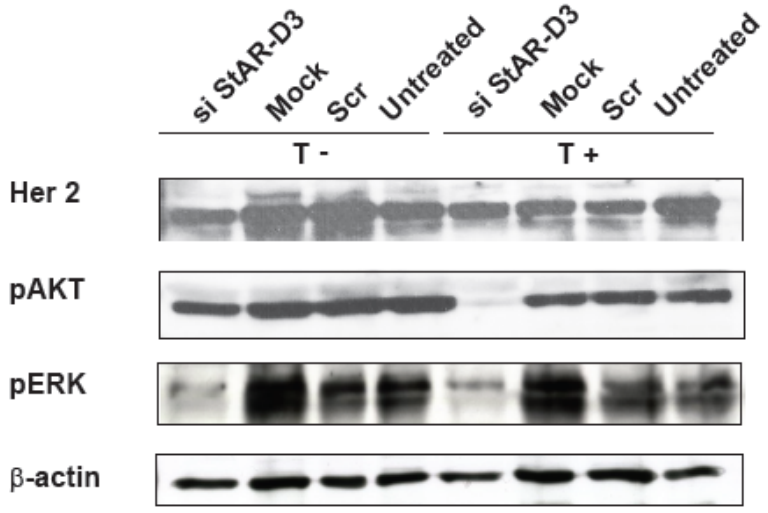



**Figure 3-11**

**Effect of StAR-D3 knockdown +/- Trastuzumab treatment on HER2 protein levels and its downstream effectors in BT474 cells.**

**Cells were reverse transfected with 20 nM pooled siRNA against StAR-D3 or a scramble sequence. T+ samples were treated with Trastuzumab 40 μg/ml for 24 hours. Equal amounts of protein were loaded in each lane and membranes were blotted with appropriate antibodies for HER2, pAKT, pERK and β-actin.**

## 3.5 Effect of StAR-D3 knockdown on Trastuzumab-resistant BT474

StAR-D3 knockdown was also carried out in Trastuzumab-resistant BT474 cells (R-BT474), following the same procedure as the native cell line. The generation and maintenance of R-BT474 cells is described in section 2.2.1.1

In R-BT474 cells, StAR-D3 knockdown caused a significant decrease in cell survival at 48 and 72 hours (Figure 3-12). This suggested that StAR-D3 also plays a role in cell survival of Trastuzumab-resistant cells and that StAR-D3 depletion is capable of inhibiting their growth.

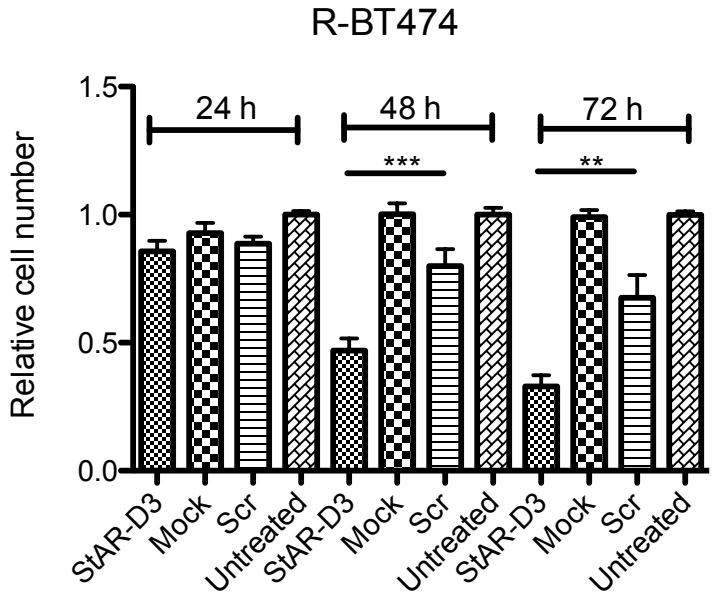



**Figure 3-12**

**Effect on cell viability by si-RNA mediated StAR-D3 knockdown in R-BT474 cells.**

**R-BT474 cells were transfected with 20 nM pooled siRNA against StAR-D3. Cell viability was assessed after 24, 48 and 72 hours respectively. Transfections were performed in triplicates and the plotted bars show the cell viability, relative to the untreated cells. Cell viability was assessed as described in section 2.2.2.**

## 3.6 Gene expression analysis on HER2 positive breast cancer patients

To further confirm the data obtained from the previous findings on cell lines and to assess the actual gene expression of StAR-D3 in a subset of HER2 positive breast cancer patients, StAR-D3 and HER2 gene expression was assessed in a retrospective series of 198 patients with early primary breast cancer. Patients characteristics are fully described by Buffa et al [60].

As described in section 2.2.15, Illumina ref8 Human array was used for the mRNA expression analysis. The analysis was performed with the help of Francesca Buffa and Laura Winchester.

Among the 198 patients considered, only 20 did not span both genes and in this subgroup the copy number was not sufficiently different. Neither of the two genes was deleted separately. These data overall confirm the co-expression of StAR-D3 and HER2 observed in preclinical analysis on HER2 positive cell lines, suggesting that the two genes are invariably co-expressed.

## 3.7 StAR-D3 staining by immunocytochemistry on BT474 cell pellet

To further characterize StAR-D3 protein expression levels and assess its prognostic value in HER2 positive breast cancer patients, BT474 cell pellet was used to optimize the staining of StAR-D3 by immunocytochemistry.

This was carried out as described in materials and methods section 2.2.14. Scramble-transfected and native BT474 were used to validate the staining and

define a correct antibody concentration for further experiments, whereas StAR-D3 knocked down BT474 cell pellet was used as a negative control. The antibodies that were previously used for StAR-D3 staining in various reports [62] [56] [63] were obtained and used for staining by immunocytochemistry. These include anti-StAR-D3 antibodies from Abcam and Novus Biologicals but none of the antibodies used was an effective tool to define correctly StAR-D3 protein expression on paraffin embedded cells as shown in the results below.

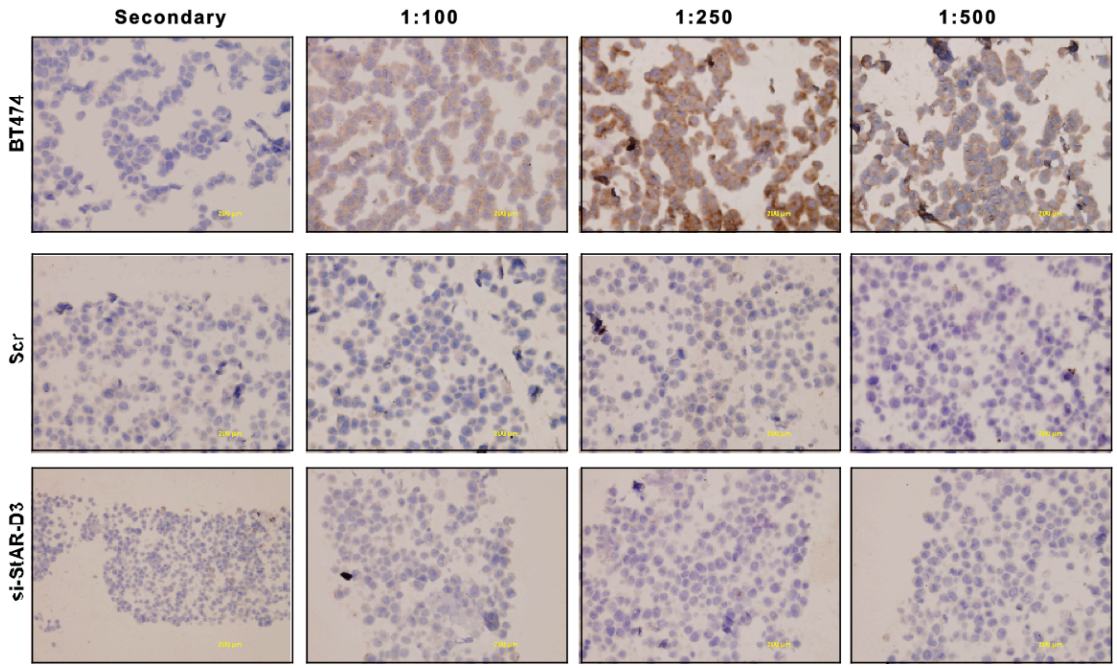



**Figure 3-13**

**BT474 cell pellet immunocytochemical staining. Upper panel shows staining of native BT474, middle panel shows staining of scramble-transfected BT474, and lower panel shows staining in StAR-D3 knockdown BT474. Primary antibody (anti-StAR-D3 Abcam antibody) concentrations are shown in the top row. Antigen retrieval was performed in Tris EDTA buffer; primary antibody conjugation was performed overnight at 4°C.**

As shown in Figure 3-13, immunocytochemical staining with Abcam anti-StAR-D3 antibody was unsuccessful and inconsistent since 1:250 concentration stained more than 1:100 in the native cell line. Most importantly, Scramble

transfected and siRNA-StAR-D3 transfected BT474 cells were equally unstained with any of the tested concentrations of primary antibody.

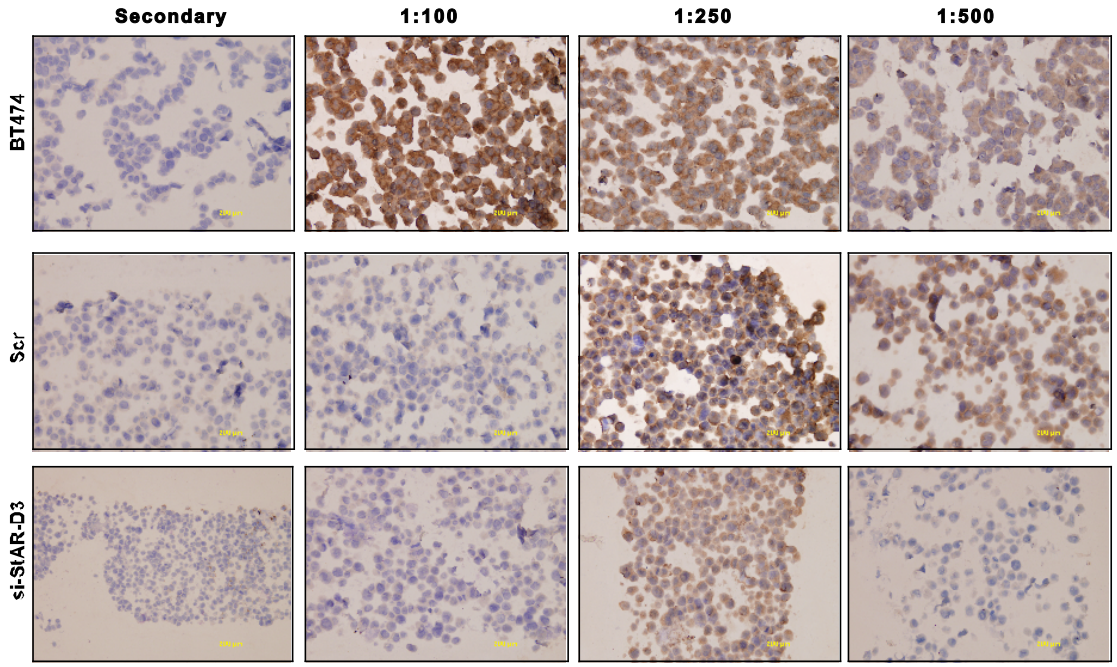



**Figure 3-14**

**BT474 cell pellet immunocytochemical staining. Upper panel shows staining of native BT474, middle panel shows staining of scramble-transfected BT474, and lower panel shows staining in StAR-D3 knockdown BT474. Primary antibody (anti-StAR-D3 Sdix) concentrations are shown in the top row. Antigen retrieval was performed in Tris EDTA buffer; primary antibody conjugation was performed overnight at 4°C.**

Figure 3-14 shows immunocytochemical staining with Sdix (Novus Biologicals) anti-StAR-D3 antibody. Despite a rather successful staining in the native BT474 cell lines (decreasing primary antibody concentration corresponded to decreased intracellular staining), overall the technique resulted in inconsistent findings. Due to non-specific staining from the antibodies, the StAR-D3 staining on human TMAs from HER2 positive breast cancer patients was not carried out.

# 4 DISCUSSION

## 4.1 StAR-D3 and HER2 expression

According to the presented data, StAR-D3 expression in HER2 amplified cell lines reflects HER2 expression, both at gene and protein level, confirming the previously published findings [59] [49].

BT474 and SKBR3 cells showed a similar pattern of expression of HER2 and StAR-D3, in contrast with MCF7 which expressed both genes at a lower extent and in which StAR-D3 protein was not detectable. This result was also confirmed by gene expression analysis in the subset of breast cancer patients considered, suggesting that HER2 and StAR-D3 are co-expressed genes.

## 4.2 StAR-D3 knockdown effects

After StAR-D3 knockdown optimization, the effects of StAR-D3 depletion were examined in terms of:

- changes of mRNA levels of genes of interest
- changes of protein levels of StAR-D3 and HER2
- changes in cell viability

StAR-D3 depletion determined a reduction in HER2 gene levels in SKBR3 and BT474 cells. In BT474, StAR-D3 knockdown also caused a decrease in HER2 protein level, suggesting its downregulation.

As far as cell survival is concerned, StAR-D3 depletion determined a significant reduction in viable cells in HER2 amplified BT474 cells. In non-HER2 amplified MCF7 cells, such decrease was not significant. The dramatic effect on the

reduction of viable cells, observed in HER2 amplified cells only, provided evidence of the role of StAR-D3 in cell survival within the subgroup of HER2 positive breast cancer, confirming previous findings by Kao et al [59].

The observed drop in cell viability in BT474 cells was partially due to increased apoptosis, since StAR-D3 depleted cells showed a higher percentage of apoptotic cells by FACS analysis.

These data suggest that StAR-D3 has a pivotal role in cell survival in HER2 positive breast cancer, and may also influence cell survival in HER2 negative cells.

## 4.3 Effect of StAR-D3 knockdown combined with Trastuzumab

Given the role of StAR-D3 knockdown on HER2 positive cell lines, the combined effect of StAR-D3 depletion with Trastuzumab treatment was analysed in order to detect any potential additive or synergistic effect. The combination of StAR-D3 depletion and Trastuzumab treatment in BT474 led to a dramatically decreased expression of pAKT level compared to either treatment alone.

In terms of cell survival, StAR-D3 depletion in combination with Trastuzumab significantly enhanced the inhibition of cell viability compared to Trastuzumab alone in BT474 cells. The synergistic effect of StAR-D3 depletion and Trastuzumab treatment, however, could not be proven since the difference in cell viability among StAR-D3 depleted and StAR-D3 depleted cells treated with Trastuzumab was not significant in any of the examined timepoints. This may be because StAR-D3 knockdown alone resulted in a dramatic reduction of cell

proliferation in these cells. In R-BT474 (Trastuzumab resistant cells), StAR-D3 depletion seemed to reverse Trastuzumab resistance. This suggests that StAR-D3 could be a novel therapeutic target in reversing resistance to Trastuzumab in HER2 positive breast cancer.

## 4.4 Conclusion and future directions

In this thesis, it was shown that the assessment of StAR-D3 expression in clinical samples was crucial both at gene and protein level. Preclinical data obtained from cell lines were further confirmed by gene expression analysis: as shown in Section 3.6**,** StAR-D3 and HER2 were invariably co-expressed in the patients data set examined, suggesting that in HER2 positive patient population StAR-D3 gene expression reflects HER2. Hence, the immunohistochemical staining and the evaluation of StAR-D3 expression on breast cancer samples was the subsequent step to further investigate a potential prognostic role of StAR-D3 as well as a predictive role within Trastuzumab treatment.

The immunocytochemical staining on cell pellet was carried out in order to assess the optimal procedure to detect StAR-D3 expression in a specific and reproducible fashion, so as to allow further analyses on clinical breast cancer samples. However, StAR-D3 staining was overall unsuccessful. Three different antibodies were used in different conditions, as described in Sections 2.1.8 and 2.2.14, but none proved to be effective and specific enough to proceed with further analyses directly on breast cancer samples. Therefore, the search for a more specific antibody to assess StAR-D3 level in breast cancer samples will be carried out by the lab in the future but unfortunately the assessment on the

prognostic role of StAR-D3 cannot be included in this thesis due to time constraints. It is anticipated that once a specific StAR-D3 antibody is found, the expression levels of StAR-D3 will be assessed in a collection of breast cancer samples (HER2 positive and negative) in relation to survival outcome of these breast cancer patients.

The data we collected provide evidence of the important role played by StAR-D3 in the maintenance of cell survival in HER2 positive breast cancer. The striking effect of StAR-D3 depletion on cell survival is the major issue on these regards. This is in accordance to previous findings in which StAR-D3 was shown to be related with poor prognosis and overall survival.

Despite these findings, however, many aspects still need to be further analysed to fully understand the functional role of StAR-D3 in breast cancer biology and its potential effects in the target therapy era (both in terms of defining Trastuzumab resistance mechanisms and in terms of providing a potential additive therapeutical target to be eventually addressed).

There are several aspects which are still in need of further investigation: the role of StAR-D3 in influencing cell survival and maintenance of malignant phenotype, along with its function within lipid metabolism pathways. Moreover, it is important to assess how StAR-D3 relates to HER2 function within lipid rafts, and to HER2 endocytosis and response to anti HER2 targeted therapy. The answers to these questions could provide a more precise picture of the role of StAR-D3 and therefore add some useful insights to breast cancer treatment.

# 5 REFERENCES


1. Baselga, J. & Swain, S.M. Novel anticancer targets: revisiting ERBB2 and discovering ERBB3. *Nat Rev Cancer* **9**, 463-475 (2009).
2. Alpy, F. & Tomasetto, C. Give lipids a START: the StAR-related lipid transfer (START) domain in mammals. *J Cell Sci* **118**, 2791-2801 (2005).
3. Yarden, Y. & Sliwkowski, M.X. Untangling the ErbB signalling network. *Nat Rev Mol Cell Biol* **2**, 127-137 (2001).
4. Hynes, N.E., Horsch, K., Olayioye, M.A. & Badache, A. The ErbB receptor tyrosine family as signal integrators. *Endocr Relat Cancer* **8**, 151-159 (2001).
5. Ignatiadis, M., Desmedt, C., Sotiriou, C., de Azambuja, E. & Piccart, M. HER-2 as a target for breast cancer therapy. *Clin Cancer Res* **15**, 1848-1852 (2009).
6. Slamon, D.J.*, et al.* Human breast cancer: correlation of relapse and survival with amplification of the HER-2/neu oncogene. *Science* **235**, 177-182 (1987).
7. Glynn, R.W., Miller, N. & Kerin, M.J. 17q12-21 - the pursuit of targeted therapy in breast cancer. *Cancer Treat Rev* **36**, 224-229 (2010).
8. Hynes, N.E. & MacDonald, G. ErbB receptors and signaling pathways in cancer. *Curr Opin Cell Biol* **21**, 177-184 (2009).
9. Zhang, X., Gureasko, J., Shen, K., Cole, P.A. & Kuriyan, J. An allosteric mechanism for activation of the kinase domain of epidermal growth factor receptor. *Cell* **125**, 1137-1149 (2006).

10. Franklin, M.C.*, et al.* Insights into ErbB signaling from the structure of the ErbB2-pertuzumab complex. *Cancer Cell* **5**, 317-328 (2004).

11. Arpino, G., Wiechmann, L., Osborne, C.K. & Schiff, R. Crosstalk between the estrogen receptor and the HER tyrosine kinase receptor family: molecular mechanism and clinical implications for endocrine therapy resistance. *Endocr Rev* **29**, 217-233 (2008).

12. Nahta, R., Yuan, L.X., Zhang, B., Kobayashi, R. & Esteva, F.J. Insulin-like growth factor-I receptor/human epidermal growth factor receptor 2 heterodimerization contributes to trastuzumab resistance of breast cancer cells. *Cancer Res* **65**, 11118-11128 (2005).

13. Baulida, J., Kraus, M.H., Alimandi, M., Di Fiore, P.P. & Carpenter, G. All ErbB receptors other than the epidermal growth factor receptor are endocytosis impaired. *J Biol Chem* **271**, 5251-5257 (1996).

14. Citri, A. & Yarden, Y. EGF-ERBB signalling: towards the systems level. *Nat Rev Mol Cell Biol* **7**, 505-516 (2006).

15. Olayioye, M.A., Neve, R.M., Lane, H.A. & Hynes, N.E. The ErbB signaling network: receptor heterodimerization in development and cancer. *Embo J* **19**, 3159-3167 (2000).

16. Mano, M.S., Rosa, D.D., De Azambuja, E., Ismael, G.F. & Durbecq, V. The 17q12-q21 amplicon: Her2 and topoisomerase-IIalpha and their importance to the biology of solid tumours. *Cancer Treat Rev* **33**, 64-77 (2007).

17. Tomasetto, C.*, et al.* Identification of four novel human genes amplified and overexpressed in breast carcinoma and localized to the q11-q21.3 region of chromosome 17. *Genomics* **28**, 367-376 (1995).

18. Kauraniemi, P., Barlund, M., Monni, O. & Kallioniemi, A. New amplified and highly expressed genes discovered in the ERBB2 amplicon in breast cancer by cDNA microarrays. *Cancer Res* **61**, 8235-8240 (2001).

19. Kauraniemi, P. & Kallioniemi, A. Activation of multiple cancer-associated genes at the ERBB2 amplicon in breast cancer. *Endocr Relat Cancer* **13**, 39-49 (2006).

20. Arriola, E.*, et al.* Genomic analysis of the HER2/TOP2A amplicon in breast cancer and breast cancer cell lines. *Lab Invest* **88**, 491-503 (2008).

21. Alpy, F.*, et al.* Metastatic lymph node 64 (MLN64), a gene overexpressed in breast cancers, is regulated by Sp/KLF transcription factors. *Oncogene* **22**, 3770-3780 (2003).

22. Hudziak, R.M.*, et al.* p185HER2 monoclonal antibody has antiproliferative effects in vitro and sensitizes human breast tumor cells to tumor necrosis factor. *Mol Cell Biol* **9**, 1165-1172 (1989).

23. Pohlmann, P.R., Mayer, I.A. & Mernaugh, R. Resistance to Trastuzumab in Breast Cancer. *Clin Cancer Res* **15**, 7479-7491 (2009).

24. Nagy, P.*, et al.* Lipid rafts and the local density of ErbB proteins influence the biological role of homo- and heteroassociations of ErbB2. *J Cell Sci* **115**, 4251-4262 (2002).

25. Spector, N.L. & Blackwell, K.L. Understanding the mechanisms behind trastuzumab therapy for human epidermal growth factor receptor 2-positive breast cancer. *J Clin Oncol* **27**, 5838-5847 (2009).

26. Clynes, R.A., Towers, T.L., Presta, L.G. & Ravetch, J.V. Inhibitory Fc receptors modulate in vivo cytotoxicity against tumor targets. *Nat Med* **6**, 443-446 (2000).

27. Piccart-Gebhart, M.J., *et al.* Trastuzumab after adjuvant chemotherapy in HER2-positive breast cancer. *N Engl J Med* **353**, 1659-1672 (2005).

28. Menendez, J.A., Vellon, L. & Lupu, R. Targeting fatty acid synthase-driven lipid rafts: a novel strategy to overcome trastuzumab resistance in breast cancer cells. *Med Hypotheses* **64**, 997-1001 (2005).

29. Mocanu, M.M., *et al.* Associations of ErbB2, beta1-integrin and lipid rafts on Herceptin (Trastuzumab) resistant and sensitive tumor cell lines. *Cancer Lett* **227**, 201-212 (2005).

30. Scaltriti, M., *et al.* Expression of p95HER2, a truncated form of the HER2 receptor, and response to anti-HER2 therapies in breast cancer. *J Natl Cancer Inst* **99**, 628-638 (2007).

31. Huang, X., *et al.* Heterotrimerization of the growth factor receptors erbB2, erbB3, and insulin-like growth factor-i receptor in breast cancer cells resistant to herceptin. *Cancer Res* **70**, 1204-1214 (2010).

32. Shattuck, D.L., Miller, J.K., Carraway, K.L., 3rd & Sweeney, C. Met receptor contributes to trastuzumab resistance of Her2-overexpressing breast cancer cells. *Cancer Res* **68**, 1471-1477 (2008).

33. Zhang, S., *et al.* Combating trastuzumab resistance by targeting SRC, a common node downstream of multiple resistance pathways. *Nat Med* **17**, 461-469 (2011).

34. Gijsen, M., *et al.* HER2 phosphorylation is maintained by a PKB negative feedback loop in response to anti-HER2 herceptin in breast cancer. *PLoS Biol* **8**, e1000563 (2010).

35. Orr, G., *et al.* Cholesterol dictates the freedom of EGF receptors and HER2 in the plane of the membrane. *Biophys J* **89**, 1362-1373 (2005).

36. Kumar-Sinha, C., Ignatoski, K.W., Lippman, M.E., Ethier, S.P. & Chinnaiyan, A.M. Transcriptome analysis of HER2 reveals a molecular connection to fatty acid synthesis. *Cancer Res* **63**, 132-139 (2003).

37. Vazquez-Martin, A., Colomer, R., Brunet, J. & Menendez, J.A. Pharmacological blockade of fatty acid synthase (FASN) reverses acquired autoresistance to trastuzumab (Herceptin by transcriptionally inhibiting 'HER2 super-expression' occurring in high-dose trastuzumab-conditioned SKBR3/Tzb100 breast cancer cells. *Int J Oncol* **31**, 769-776 (2007).

38. Alpy, F. & Tomasetto, C. MLN64 and MENTHO, two mediators of endosomal cholesterol transport. *Biochem Soc Trans* **34**, 343-345 (2006).

39. Alpy, F., Legueux, F., Bianchetti, L. & Tomasetto, C. [START domain-containing proteins: a review of their role in lipid transport and exchange]. *Med Sci (Paris)* **25**, 181-191 (2009).

40. Soccio, R.E. & Breslow, J.L. StAR-related lipid transfer (START) proteins: mediators of intracellular lipid metabolism. *J Biol Chem* **278**, 22183-22186 (2003).

41. Miller, W.L. Steroidogenic acute regulatory protein (StAR), a novel mitochondrial cholesterol transporter. *Biochim Biophys Acta* **1771**, 663-676 (2007).

42. Stocco, D.M. StARTing to understand cholesterol transfer. *Nat Struct Biol* **7**, 445-447 (2000).

43. Miller, W.L. StAR search--what we know about how the steroidogenic acute regulatory protein mediates mitochondrial cholesterol import. *Mol Endocrinol* **21**, 589-601 (2007).

44. Christenson, L.K. & Strauss, J.F., 3rd. Steroidogenic acute regulatory protein (StAR) and the intramitochondrial translocation of cholesterol. *Biochim Biophys Acta* **1529**, 175-187 (2000).

45. Tsujishita, Y. & Hurley, J.H. Structure and lipid transport mechanism of a StAR-related domain. *Nat Struct Biol* **7**, 408-414 (2000).

46. Lamy, P.J.*, et al.* Quantification and clinical relevance of gene amplification at chromosome 17q12-q21 in human epidermal growth factor receptor 2-amplified breast cancers. *Breast Cancer Res* **13**, R15 (2011).

47. Kao, J.*, et al.* Molecular profiling of breast cancer cell lines defines relevant tumor models and provides a resource for cancer gene discovery. *PLoS One* **4**, e6146 (2009).

48. Strauss, J.F., 3rd, Kishida, T., Christenson, L.K., Fujimoto, T. & Hiroi, H. START domain proteins and the intracellular trafficking of cholesterol in steroidogenic cells. *Mol Cell Endocrinol* **202**, 59-65 (2003).

49. Moog-Lutz, C.*, et al.* MLN64 exhibits homology with the steroidogenic acute regulatory protein (STAR) and is over-expressed in human breast carcinomas. *Int J Cancer* **71**, 183-191 (1997).

50. Alpy, F.*, et al.* The steroidogenic acute regulatory protein homolog MLN64, a late endosomal cholesterol-binding protein. *J Biol Chem* **276**, 4261-4269 (2001).

51. Kobayashi, T.*, et al.* A lipid associated with the antiphospholipid syndrome regulates endosome structure and function. *Nature* **392**, 193-197 (1998).

52. Watari, H., *et al.* MLN64 contains a domain with homology to the steroidogenic acute regulatory protein (StAR) that stimulates steroidogenesis. *Proc Natl Acad Sci U S A* **94**, 8462-8467 (1997).

53. Rigotti, A., Cohen, D.E. & Zanlungo, S. STARTing to understand MLN64 function in cholesterol transport. *J Lipid Res* **51**, 2015-2017 (2010).

54. Kishida, T., *et al.* Targeted mutation of the MLN64 START domain causes only modest alterations in cellular sterol metabolism. *J Biol Chem* **279**, 19276-19285 (2004).

55. Holtta-Vuori, M., *et al.* MLN64 is involved in actin-mediated dynamics of late endocytic organelles. *Mol Biol Cell* **16**, 3873-3886 (2005).

56. Cai, W., Ye, L., Sun, J., Mansel, R.E. & Jiang, W.G. Expression of MLN64 influences cellular matrix adhesion of breast cancer cells, the role for focal adhesion kinase. *Int J Mol Med* **25**, 573-580 (2010).

57. Vinatzer, U., *et al.* Expression of HER2 and the coamplified genes GRB7 and MLN64 in human breast cancer: quantitative real-time reverse transcription-PCR as a diagnostic alternative to immunohistochemistry and fluorescence in situ hybridization. *Clin Cancer Res* **11**, 8348-8357 (2005).

58. Stigliano, A., *et al.* Increased metastatic lymph node 64 and CYP17 expression are associated with high stage prostate cancer. *J Endocrinol* **194**, 55-61 (2007).

59. Kao, J. & Pollack, J.R. RNA interference-based functional dissection of the 17q12 amplicon in breast cancer reveals contribution of coamplified genes. *Genes Chromosomes Cancer* **45**, 761-769 (2006).

60. Buffa, F.M., *et al.* microRNA-associated progression pathways and potential therapeutic targets identified by integrated mRNA and microRNA expression profiling in breast cancer. *Cancer Res* **71**, 5635-5645 (2011).

61. Yau, C., *et al.* A statistical approach for detecting genomic aberrations in heterogeneous tumor samples from single nucleotide polymorphism genotyping data. *Genome Biol* **11**, R92 (2010).

62. http://www.proteinatlas.org/.

63. Bonuccelli, G., *et al.* Caveolin-1 (P132L), a common breast cancer mutation, confers mammary cell invasiveness and defines a novel stem cell/metastasis-associated gene signature. *Am J Pathol* **174**, 1650-1662 (2009).